

Response to the Referees

We thank the four reviewers for all the comments on the manuscript. A response to all of the comments are found in the following sections. The comments from the Referees are written in a grey, italic font, followed by our response written in black. The page and line numbers for the changes refers to the revised manuscript with track changes in the end of this document. A complete list of references is also found in this revised manuscript.

Response to Referee #1

“Diurnal Cycle of NO₃. The paper identifies the increase in NO₃ between the preindustrial and the present day as the major change in oxidants. This is most likely true. However, their model treats NO₃ in a relatively unsophisticated manner. The text explicitly says that OH and HO₂ concentrations have a diurnal cycle imposed on them whereas NO₃ is not mentioned suggesting that it does not. In reality NO₃ does have a significant diurnal cycle. Its rapid photolysis leads to low concentrations during the day and high during the night. Thus, in the real atmosphere NO₃ anti-correlates with isoprene and monoterpenes (this depends to an extent upon the monoterpene speciation) thus NO₃ likely only plays a minor role in the oxidation of these species. By not having a diurnal cycle in the NO₃ concentration this anti-correlation is lost in the model which then likely favours the NO₃ oxidation route over the other oxidations routes. Given the central importance of NO₃ to the primary conclusion of the paper this lack of anti-correlation provides significant problem that needs to be resolved before the paper can go forwards to publication.”

It is correct that our model does not have a diurnal cycle for NO₃, and we agree that it should. The diurnal cycles for OH and HO₂ were already implemented in the model when this study was started up. The lack of a diurnal cycle for NO₃ was discovered after the main simulations for this study were carried out. As a solution to this issue, we have added an extra sensitivity test (from p.13, l.24) where a diurnal cycle to NO₃ is applied. The result of this test shows that the lack of this diurnal cycle in the original setup only slightly impacts the result of this study, so we are keeping the original default setup in this study as it is. The main reason for the minor impact of the diurnal cycle of NO₃ is that the main effect of NO₃ is oxidation of DMS over the oceans. Since the lifetime of DMS is 36 and 55 hours (present-day and preindustrial respectively), the reduction in the nighttime oxidation when not applying a diurnal cycle will have time to be compensated by an increase in the daytime oxidation.

“Attribution of impacts The chemistry scheme in the model is fundamental to the magnitude of the impacts simulated. There is little explanation for the choice of yield from the VOCs or DMS. A section explaining these choices and previous work to justify these choices would be useful.”

We agree. More information about the yields applied in CAM5.3-Oslo are now included in the model description of this manuscript (p.5, l.12-19). We acknowledge the fact that the yields are uncertain. For both monoterpene and isoprene, the yields are within the range found in other global models and from laboratory experiments (Kroll et al., 2005; Lee et al., 2006; Dentener et al., 2006; Spracklen et al., 2011; Tsigaridis, 2014, Jokinen et al., 2015). Other global models with simplified tropospheric chemistry often do not trace MSA (Neale et al., 2012; Tsigaridis et al., 2014), assuming a yield factor of 0, but since several studies have shown that MSA can contribute to aerosol formation and growth, CAM5.3-Oslo keeps MSA as SOA_LV and SOA_SV in the model after oxidation (Bork et al., 2014; Willis et al., 2016; Chen and Finlayson-Pitts, 2017). The choice of the yields and the ratio between the two are unknown. For that reason, we emphasize the importance of the models representation of DMS-oxidation by the two sensitivity tests in the end of the paper (p.12, l.21-34) where we see how the result is affected if we assume that

1. none of the MSA can contribute to nucleation (NOSOALVDMS, which corresponds to a yield factor for SOA_SV of 100 % and a yield factor for SOA_LV of 0 %)
2. none of the MSA can contribute to either nucleation nor condensation (NOSOAA, which corresponds to a yield factor of 0 % for both SOA_SV and SOA_LV).

As shown, the magnitude of the effect on the total aerosol indirect effect by changing the oxidant level is highly dependent on getting some SOA out of the DMS-oxidation reaction that can condense (NOSOAA), but it is not that dependent on SOA that can nucleate (NOSOALV). This is specified in the section with the results from the sensitivity tests and in the conclusions (p.15, l.6-8). As part of another research project (BACCHUS - impact of Biogenic versus Anthropogenic emissions on Clouds and Climate: Towards a Holistic UnderStanding), the model applied in this study is taking part in an intercomparison where the choice of yields for the oxidation reactions involving BVOC is studied through several sensitivity tests, but this is beyond the scope of this study.

*“There are couple of ways that the change in oxidants could impact the oxidation of the precursor compounds, and so the production of low volatile products. They could change the net yield of compound (SOA.SV vs SOA.LV), or they could change the location of the oxidation. It would be useful to know which process is occurring here. Given that the yield of SOA.SV is the same for all isoprene oxidation routes, any change in the cloud-aerosol feedback due to isoprene can only be occurring because of the change in the location of oxidation - the globally total production of SOA.SV from isoprene is the same in all simulations ($0.15 * \text{total isoprene emission}$).*

Monoterpenes behave differently. Oxidation by O₃ leads to the production of SOA.LV whereas oxidation by other methods leads to SOA.SV. Here a change in the oxidant may lead to significant changes in the production of the different SOA times. A similar change might occur with DMS oxidation. The authors attribute all of the changes they see to changes in the location of the oxidation, but they don't really give much evidence to support this.

We agree that both changes in the location of the oxidation and changes in the net yield of the compounds can contribute to the results in this study. Since the sensitivity tests NOSOALVDMS and NOSOALVBVOC (p.12, l.21-34) show that a shift towards more production of low volatile SOA has a negligible effect on the main result in this study, the attention has been on the changes in the location of the oxidation. With that said, it was not our intention to attribute all of the changes we see to this location change. In fact, the results from the sensitivity test NOSOA (p.13, l.1-14) show a shift towards more production of condensate relative to the production of new particles, which makes it easier for the droplets to activate, also has a big impact on the result. This was highlighted in the section containing the summary and conclusions (p.15, l.6-8). When it comes to the section about the increase in the aerosol number concentration, we agree that the change in the net yield of the compounds could be highlighted more. We have now rewritten this section in an attempt to emphasize this effect (from p.8, l.4 to p.10, l.2), including a table (Table 5) showing how the conversion rates for all the oxidation reactions change when we change the oxidant level.

Figure 9 shows the change in the fractional oxidation as a function of height, but this doesn't show in absolute terms how much of the precursor is oxidized in different places. This is a little misleading - very little of the monoterpene / isoprene is oxidised in the upper troposphere compared to the lower troposphere. Perhaps showing the absolute change in oxidation would help with this? This would probably need to be on a log scale."

We agree that most of the precursor gases are oxidized in the boundary layer. To emphasize this, we have added another panel to each part of Fig. 7 (corresponding to Fig. 9 in the old manuscript) showing how much of the specie is oxidized at each level compared to the level where most of the specie is oxidized.

"It would be useful to have a table or figure which shows how much H₂SO₄, SOA.LV, and SOA.SV is produced globally by each route for each simulation."

We agree. This is now included in Table 5 and discussed in the section about the aerosol number concentration (Sect. 4.11, from p.8, l.4 to p.10, l.2).

"Given the length of the description of the impact on the aerosol and clouds there should be an increase in the description of how the chemistry is making this impact. This explanation of why the emissions are changing the SOA.LV, SOA.SV and H₂SO₄ tracers is somewhat weak"

We hope that the inclusion of Table 1 and Table 5, the different sensitivity tests (including the new test with a diurnal cycle for NO₃), the extended discussion in Sect. 4.1.1 and the inclusion of Fig. 7 and the corresponding text is satisfactory.

“Can the total mass of isoprene and monoterpene be included into a table somewhere? The MEGAN scheme can lead to significantly varying emissions depending upon the implementation into the transport model. It would be useful to know these values.”

We agree. It's now included in Table 1.

“It would also be useful to state that the assumption all of the mono-terpene emission is considered to be alpha-pinene which seems to be the implication of the rate constants chosen.”

Yes, it is correct that all of the monoterpene is considered to be alpha-pinene. This is now added to the manuscript (p.5, l.16).

“The chemistry scheme also doesn't seem to include aqueous SO₂+H₂O₂. Although this is occurring within the cloud phase it is still a chemical reaction and for completeness I think it should be included.”

Yes, it does. This is specified in the manuscript (p.5, l.16). To what extent the aqueous phase oxidation reactions change with the switch from PD- to PI-oxidants can also be seen in Fig. 7(b).

“Figure 9: Figure Caption. The language in the figure caption should be re-examined as it doesn't make sense”

We agree. A new caption is added. (This figure is now called Fig. 7).

Response to Referee #2

“It would be useful to see a bit more discussion on the extent to which we can know what pre-industrial oxidant levels actually were (or the challenges in determining them). The authors point out that a number of studies have attempted to infer pre-industrial oxidant levels from emissions inventories (also uncertain) and limited observations, but a bit more detail here about what is known and how well would be useful context.”

Limited observations refers to simple measurements of surface ozone from a few European stations (Montsouris and Pic DuMidi) in the late 19th century (Volz and Kley, 1988). We have added a sentence about how well the prescribed O₃ used in this study corresponds to measured O₃ at the Montsouris station in Volz and Kley (1988) (p.5, l.28-30). For the very reactive radicals NO₃ and OH, there are no historical measurements. Thus, the PI levels have to be estimated by

models. However, we can have some confidence in these models when they are tested against current observations (e.g. as in Khan et al., for NO₃).

We have added a few sentences about the comparison of model simulated concentrations with PD-observations in Sect. 2.2 (p.5, l.31-35).

“Relating to my previous point - since there can only be limited confidence in any simulated pre-industrial oxidant levels, one possibility would be to consider how well the full-chemistry model captures present-day oxidant concentrations in clean v. polluted regions. Without this, the paper makes an important point about the potential impact of incorrect / inappropriate oxidant concentrations when diagnosing RFs, but doesn't necessarily tell us how much we can trust this particular set of pre-industrial oxidants and therefore the size of the change in RF that is diagnosed.”

We agree with the reviewer that: "Without this, the paper makes an important point about the potential impact of incorrect / inappropriate oxidant concentrations when diagnosing radiative forcings, but does not necessarily tell us how much we can trust this particular set of pre-industrial oxidants and therefore the size of the change in RF that is diagnosed."

The key process identified in our work is the change in oxidation of DMS by NO₃. There are a few observations of NO₃ from marine sites (Brown and Stutz, 2012). However, most if not all of these are from coastal regions and often in the outflow of major industrialized regions in the northern hemisphere. Thus, measurements of NO₃ from the more remote Pacific region that we find is the most important is lacking. On the positive side, the lack of knowledge of PI-levels of NO₃ in these regions are probably not very important since they were anyhow very low. Thus, a key factor would be to go out and measure the current levels during the season of DMS production.

When it comes to the other oxidants, we have added a few sentences in Sect. 2.2 (p.5, l.31-35) about how good agreement it is between observations from PD and modeled PD-values of OH and O₃ by a full-chemistry model that is almost identical to the model that produced the oxidant fields applied in this study.

“Could you add more detail on the new particle formation mechanism that is used in OsloAero? This is also an important factor in determining PI particle concentrations, and therefore the PI to PD radiative forcing. For example, Gordon et al., (2016) found that including pure biogenic new particle formation reduced the strength of their simulated PI to PD first aerosol indirect RF.”

We agree that this is an important factor. More information about the new particle formation is added to the model description in Sect. 2 (p.4, l.19-24). We have also added a few sentences

about the lack of pure biogenic new particle formation in the section containing the summary and conclusions, Sect.5 (p.14, l.23-24).

“Minor / technical remarks:

p6, line 29: change to “low volatility””

Done

“p7, line 21: change to “describes” p7, “

Done

“line 26: change to “increases” p7, “

Done

“line 28: correct the spelling of “switching” “

Done

“p8, line 14-15: rephrase the sentence starting “Figure 9”, may require insertion of an “is” somewhere?”

Done

“p8, line 17: should this just be Figure 9(a)? (since (c) and (d) do not relate to DMS?)”

Done

“p8, line 18-20: I think here you are saying that reaction R2 + R3 is favoured over R4 since there is less oxidation via the NO3 pathway – rephrase to avoid saying “..out off a DMS-“”

Done

“p11, line 9: change to “gives””

Not changed. “The results give”.

“Figure 8: what is meant by “aerosol size” in this Figure? Would be useful to describe in the caption”

This was described in the text: “the mean size of the aerosols is calculated as a mean of the number mean radius of all mixtures in the model, weighted by the number of aerosols in each mixture”. The explanation is now moved to the caption of the figure instead (Now called Fig. 9).

“Figure 9: rephrase third sentence of the caption”

Done. (Now called Fig. 7)

“Table 5: is there an error here in the description of the NOSOA simulation? (the reaction is the same as the line above)”

Yes. That was an error. This is now corrected. (Now called Table 7)

Response to Referee #3

1. The preindustrial oxidant fields are from Lamarque et al., 2010. Is it correct to assume that these oxidant fields were generated without on-line aerosol-cloud radiative interactions i.e. this preindustrial gas-phase chemistry does not “see” the brighter preindustrial clouds found in the present study with CAM5.3-Oslo? This question has broader implications. The changes in aerosol-cloud interactions and associated meteorology in PI versus PD state will have an influence on the resultant oxidant levels, not least through altering photolysis rates. How does the application of off-line oxidants here versus fully 2-way coupled on-line oxidants affect the main results?

Yes, it is correct that these fields have been generated with a model without online aerosol-cloud radiative interactions, so the gas-phase chemistry is not affected by the brighter PI-clouds we get in this study. We have now pointed out this problem in the summary and conclusion part of the manuscript in Sect. 5 (p.15, l.25-29). This study is the first to highlight the importance of correct treatment of gas-aerosol interactions through oxidation when modeling aerosol indirect effects and the first to address the issue of applying the same oxidant level to both preindustrial and present-day precursor gases. We think that including second-order effects linked up to two-way coupled simulations should be a focus for upcoming studies, as well as applying different kind of input datasets for the oxidants generated by more advanced models, but that this is beyond the scope of this paper.

2. It is not clear how long the simulations are run for in total?

The nudged simulations are run for four years, but they are started from simulations with free meteorology using the same oxidant concentrations and the same aerosol concentrations. We have tried to specify this better in the manuscript (p.6, l.19-23).

However, it is reported that the last 3 years of the run are used for the analyses. ERF allows all feedbacks between land-atmosphere and the land-atmosphere system to come into steady-state

with the imposed radiative perturbation. Is the land-atmosphere system in steady-state after only 3 years of running the model? Many of the global chemistry-climate model frameworks seem to run for much longer (even with fixed SSTs and sea ice) to allow for the land-atmosphere system to come into steady-state i.e. more than 20 years.

It is correct that only the last three years of the four years simulations are analyzed. The standard error for the total aerosol indirect effect for these three years is only 0.01 W/m². Sensitivity simulations (not shown in this paper) show that modeling the total aerosol indirect effect using nudging for 11 years, analyzing the last ten, gives the same result as only running for four years and analyzing the last three, and there is no drift in the signal. Since producing and storing six hourly meteorological data with three dimensions (pressure level, latitude, longitude) and running all the sensitivity tests in this study is computationally expensive, we've chosen to not extend the simulations. This information is now included in the manuscript (p.6, l.23-27). For even more complementary answer to the question about steady-state: see the end of the answer to the next comment.

3. Is it methodologically correct to 'nudge' a simulation and calculate ERF?

According to the definition of ERF in IPCC AR5, we acknowledge that nudging the winds is not a 100 % correct method to calculate ERF, since the fast feedbacks on the winds due to aerosol changes are missing and since we do not conserve momentum when replacing ~8 % of the wind signal (similar to a relaxation time scale of six hours) each timestep by a prescribed wind field from another simulation. Since this study consists of several model setups, all with three different simulations each, the computational cost of running all of them with free meteorology will be too high. Since this study is the first to address the issue of using PD-oxidants for both simulations, we think that the tests where we look at the effect of changing one oxidant at a time and the rest of the sensitivity tests are all important for examining the impact of historical oxidant changes on the PD-PI aerosol indirect effect. This would not be affordable for us to do without the use of nudging. Nevertheless, we acknowledge that this issue should be addressed in the paper, so we have added one extra sensitivity test where we run the three simulations from the original default model setup (PDAERO+PDOXI, PIAERO+PDOXI and PIAERO+PIOXI) all over again, but with free meteorology for 50 years each (p.14, l.6-21). Even after 50 years, the uncertainty due to natural variability is large, but the resulting change in the total aerosol indirect effect due to historical oxidant changes falls in the same range for the nudged configuration as for the free running, indicating that the error in the modeled ERF due to nudging is not changing the main results. Related to the previous comment about steady-state, analyzing only the last 30 years of the simulations with free meteorology gives the same result for the total aerosol indirect effect and for the change due to historical oxidant changes as when analyzing the last 50 years, indicating that there is no drift in the signal. This is also pointed out in the manuscript (p.14, l.20-21).

4. Is it possible to use the 3 model run years to generate a standard error estimate of uncertainty based on interannual internal variability – thus not providing naked numbers e.g. -1.32 W/m² and -1.07 W/m². The numbers may appear somewhat meaningless within the context of ERF_{aci} without any uncertainty range information.

The standard error of the three years with nudging is only 0.01 W/m². We think that adding this uncertainty to the results in this study might give an impression for the readers that the uncertainty linked to historical oxidant changes are low, which is not the case. The uncertainties are high, not only due to interannual variability, but mainly due to other factors that are discussed in the paper (lack of information about PI-oxidant concentrations, simplified model chemistry, uncertainties in yields and more). But we have added standard errors to the modeled total aerosol indirect effect from the new sensitivity test “FREEMET” so the readers can see the magnitude of the interannual variability (p.14, l.17).

5. Does the preindustrial simulation include a preindustrial land cover map? A few recent studies show a substantial net decrease in BVOC emissions between preindustrial and present day due to the historical cropland expansion (e.g. Heald et al., 2016; Unger, 2013). Temperate zone forests and grasses have been replaced with crops and pasture that represents a loss of BVOCs from the Earth system. The PI-PD SOA and cloud changes are sensitive to the BVOC emission changes. How will the results be affected in the case of higher PI BVOC emissions?

No, all of the simulations are run with the same land cover map from PD to avoid the result to be impacted by different surface albedos and heat fluxes between the simulations performed with PD- and PI-aerosol emissions. We agree that this also results in almost identical emissions of BVOC (and dust) in the two eras. We are currently preparing another manuscript based on a study of how different kinds of natural emissions have changed since PI due to anthropogenic activities, and how this affects the PD-PI aerosol indirect effect. Preliminary results show that the higher BVOC-emissions in the PI-era due to changes in land cover results in less negative total aerosol indirect effect of ~0.10 W/m². We have yet to test how these emission changes will affect the PD-PI aerosol indirect effect when applying PI-oxidants to the PI-simulation. The lack of differences in many kind of emissions (including BVOC) between the two eras are already mentioned in the summary and conclusion part of the manuscript (from p.15, l.33 to p.16, l.4).

In turn, the higher PI BVOC emissions will influence oxidant levels (reducing them further?). It is unlikely that the higher PI BVOC emissions were included in the oxidant simulations in Lamarque et al., 2010.

Yes, we agree that higher BVOC-emissions in PI probably will results in reduced concentrations of the PI-oxidants, especially in the high BVOC-emission regions. The simulations in Lamarque et al. (2010) include prescribed BVOC-emissions, but they are the same for both eras. More recently

developed model versions that will be applied in CMIP6 (like NorESM2, based on CAM6-Oslo) will have prescribed oxidant concentrations produced by a more developed model that probably will see different BVOC-emissions in the two eras due to different land cover maps, and also include online aerosol-cloud radiative interactions (as mentioned in the previous comment). This model version of CAM-Oslo is not yet finalized and ready to be used in this study. It will be interesting to carry out some of the simulations in this study all over again with the CMIP6-models to see how the more developed models will impact the result, but this is beyond the scope of this paper.

6. Δ_{clean} from Ghan (2013) is introduced on Page 4. Readers from gas-phase chemistry community may appreciate a bit more explanation here (1-2 sentences) on the meaning of Δ_{clean} .

We agree. Some extended information about this term is added to the model description (p.4, l.29-31).

Response to Referee #4

The authors note that the major driver leading to brighter clouds in the preindustrial period compared to default oxidant assumptions is the nitrate radical level. Since the nitrate radical is most abundant at night while daytime oxidation is dominated by OH and ozone, have the authors thought about their results in the context of this diurnal shift towards daytime oxidation? Is the change in AIE mostly due to changes in daytime aerosols? What does that mean if the major oxidant driving changes is primarily nocturnal? Is nitrate radical oxidation most confined to the lowest model layers as a result of nocturnally stable boundary layers? Thus do the changes in vertical profiles of monoterpenes and DMS in figure 5 mostly reflect an increase in near-surface nocturnal concentrations with PI oxidants? Do any results (Table 3 compound lifetimes?) need to be presented as a daytime average instead of 24-hour average?

Since Fig. 3 shows that the changes in the total aerosol indirect effect mainly are results of the effect on the shortwave radiation, it is the daytime aerosol concentration and the daytime cloud properties that are most important. As replied to Referee #1, the model applied in this study unfortunately does not include a diurnal cycle for NO₃. This means that the oxidation capacity of NO₃ is the same both day and night, and that the oxidation rates will only vary due to the diurnal cycle of some of the emissions (BVOC, but not DMS and SO₂). We have added a sensitivity test, DIURNALNO₃ (from p.13, l.23), which shows that the main result of this study is not affected by adding a diurnal cycle to the NO₃-concentrations. To be able to present different quantities like concentrations, lifetimes and reaction rates as daytime and nighttime averages, all simulations would have to be redone with more frequent output (we only have monthly mean output of these quantities at the moment). Based on the results from the DIURNALNO₃-test, we do not think that separate daytime and night-time averages would offer any additional insights important enough to justify the extra work, cost and time that they would require.

Minor comment: Page 8, line 20: "SO₂ nucleates easier than SOA" Is SO₂ the model species that nucleates due to logistical reasons or is it sulfuric acid?

It should be H₂SO₄, not SO₂. This is now corrected (p.10, l.26).

Strong impacts on aerosol indirect effects from historical oxidant changes

Inger Helene Hafsaahl Karset¹, Terje Koren Berntsen^{1,2}, Trude Storelvmo¹, Kari Alterskjær², Alf Grini⁴, Dirk Olivie⁴, Alf Kirkevåg⁴, Øyvind Seland⁴, Trond Iversen⁴, and Michael Schulz⁴

¹University of Oslo, Department of Geosciences, Section for Meteorology and Oceanography

²CICERO Center for International Climate Research, Oslo, Norway

⁴Norwegian Meteorological Institute, Oslo, Norway

Correspondence to: Inger Helene Hafsaahl Karset (i.h.h.karset@geo.uio.no)

Abstract. Uncertainties in effective radiative forcings through aerosol-cloud interactions (ERF_{aci} , also called aerosol indirect effects) contribute strongly to the uncertainty in the total preindustrial-to-present-day anthropogenic forcing. Some forcing-estimates of the ~~aerosol indirect effects~~ total aerosol indirect effect are so negative that they even offset the greenhouse gas forcing. This study highlights the role of oxidants in modeling of ~~the~~ preindustrial-to-present-day aerosol indirect effects. We argue that the aerosol precursor gases should be exposed to oxidants of its era to get a more correct representation of secondary aerosol formation. Our model simulations show that the total aerosol indirect effect changes from -1.32 Wm^{-2} to -1.07 Wm^{-2} when the precursor gases in the preindustrial simulation are exposed to preindustrial instead of present-day oxidants. This happens because of a brightening of the clouds in the preindustrial simulation, mainly due to large changes in the nitrate radical (NO_3). The weaker oxidative power of the preindustrial atmosphere extends the lifetime of the precursor gases, enabling them to be transported higher up in the atmosphere and towards more remote areas where the susceptibility of the cloud albedo to aerosol changes is high. The oxidation changes also shift the importance of different chemical reactions and produce more condensate, thus increasing the size of the aerosols and making it easier for them to activate as cloud condensation nuclei.

1 Introduction

It is well established that changes in atmospheric aerosol abundance since ~~pre-industrial~~ preindustrial times have had a strong, albeit uncertain, influence on Earth's climate over the last century. Atmospheric aerosols are not just impacting climate by directly absorbing and reflecting radiation, but also indirectly by acting as cloud condensation nuclei (CCN) and ice nuclei (IN). Through cloud albedo increases mediated by enhancements of CCN, aerosols brighten the clouds and enhance their cooling effect by increasing the reflection of incoming solar radiation (Twomey, 1977). More numerous cloud droplets may also alter rain formation mechanisms, thus the cooling effect could be further enhanced by suppressed precipitation followed by increased cloud lifetime, cloud amount and cloud extent (Albrecht, 1989; Pincus and Baker, 1994). The impact of IN changes remains uncertain (Storelvmo, 2017; Lohmann, 2017).

Aerosol indirect effects on Earth's radiation budget are often quantified in terms of their effective radiative forcing (Myhre et al., 2013). Unlike instantaneous radiative forcing, effective radiative forcing includes effects from rapid tropospheric ad-

justments (Boucher et al., 2013). Otherwise, it does not include any feedbacks in the climate system. Model studies of ~~the~~ direct and indirect effects typically carry out two simulations, with aerosols and aerosol precursor gases from preindustrial times (PI) and present-day (PD), respectively. The difference in cloud forcing, measured as effective radiative forcing between the two simulations, represents the ~~aerosol indirect effects~~ total aerosol indirect effect if the direct aerosol effect in cloudy skies is negligible (Ghan, 2013). Results from several model studies show that this number varies considerably. To what extent aerosol-cloud interactions have contributed to the global radiative forcing in the anthropocene remains highly uncertain and continues to be a research topic of much interest. ~~(Lohmann, 2017)~~ Lohmann (2017) shows that model estimates of $ERF_{ari+aci}$ (ari: aerosol-radiation interactions, aci: aerosol-cloud interactions) vary from -0.07 to -3.41 Wm^{-2} , while the ~~latest fifth~~ Assessment Report (AR5) from the Intergovernmental Panel on Climate Change (IPCC) gives an expert judgement of $ERF_{ari+aci}$ of -0.9 Wm^{-2} , with a 5 to 95 % uncertainty range of -1.9 to -0.1 Wm^{-2} mostly coming from the uncertainties in the aci-component (Boucher et al., 2013). Uncertainties in the natural background emissions have been highlighted as a large contributor to the uncertainty in the indirect effects (Lohmann et al., 2000; Kirkevåg et al., 2008; Hoose et al., 2009; Carslaw et al., 2013), while Gettelman (2015) pointed out that its sensitivity to parameterizations of microphysical processes in global models ~~are~~ is even higher. In this study, we examine a third factor, namely the oxidants involved in ~~forming the formation of~~ aerosols.

Aerosols may enter the atmosphere directly, or they can be formed after in situ oxidation of precursor gases to condensable species (Seinfeld and Pandis, 2016). The oxidation process yields secondary gases with lower saturation vapor pressure, which allows them to either condense on already existing particles or nucleate into new particles under atmospheric conditions. Both processes depend on the amount of emitted precursor gases, but also on the atmospheric oxidation capacity. While model studies of PD-PI aerosol indirect effects usually point out that they use different emissions of aerosols and aerosol precursor gases for the two different time periods, the choice of oxidant levels is usually not specified (Lohmann and Diehl, 2006; Menon and Rotstain, 2006; Hoose et al., 2008; Storelvmo et al., 2008; Lohmann, 2008; Lohmann and Ferrachat, 2010; Wang et al., 2011; Yun and Penner, 2013; Neubauer et al., 2014; Gettelman, 2015; Gettelman et al., 2015; Tonttila et al., 2015; Sant et al., 2015). A notable exception is Salzmänn et al. (2010), who use different oxidant levels for the different eras. Personal communication with scientists from different ~~modelling~~ modeling groups confirms that it is common to use PD-oxidants for both ~~PD and PI simulations~~ PD- and PI-simulations (U. Lohmann, C. Hoose, A. Kirkevåg, A. Gettelman, D. Neubauer, personal communication, 2017).

Human activity has influenced the oxidant level mainly through increased emissions of CO, NO_x, and CH₄ from fossil fuel combustion, biomass burning and the use of fertilizers in agriculture (Crutzen and Lelieveld, 2001). Due to this anthropogenic activity, precursor gases emitted into the ~~PI-atmosphere~~ PI-atmosphere were exposed to a different oxidant level than the gases emitted today, implying a difference in the rate and distribution of new particle formation in the atmosphere. The aim of this study is to quantify this difference and to give a more realistic estimate of the total PD-PI aerosol indirect effect by letting the precursor gases in the PI-simulation (the simulation with emissions of aerosols and aerosol precursor gases from PI) be exposed to an oxidant level that is representative for its era.

Due to counteracting effects, the sign and magnitude of the global mean historical oxidant change is uncertain (Naik et al., 2013a, b; Murray et al., 2014). While in a low NO_x-regime, CO and CH₄ act as sinks for the hydroxyl radical (OH), one of the most important oxidants in the troposphere, the opposite is the case in a high NO_x-regime (Collins et al., 2002). As a consequence, OH has experienced an increase in polluted areas where the NO_x level is high, while it has decreased in remote areas where the NO_x-level is low and the CH₄ level is high due to their different lifetimes (Wang and Jacob, 1998; Prinn, 2003). The situation is different for ozone (O₃), where an increase in NO_x, CO or CH₄ usually favours O₃-production in both low and high NO_x regimes (Seinfeld, 1989; Chameides et al., 1992). This also holds for the NO₃ radical, which is produced through reactions between NO_x and O₃ (Wayne et al., 1991) and probably was present at lower levels everywhere in preindustrial times.

Difficulties in measuring the oxidants directly from the atmosphere and the lack of information about oxidants in sediments and ice cores has resulted in limited information about the atmospheric oxidant level, ~~especially~~ (Pavelin et al., 1999). This is especially the case for the time period before the industrial era (Pavelin et al., 1999), where it is limited to simple measurements of surface ozone from a few European stations (Volz and Kley, 1988). Despite this limitation, results from model simulations based on information about emission changes, in combination with the few oxidant measurements that exist, give an indication of how the oxidative power of the atmosphere has changed since preindustrial time (Prinn, 2003; Berntsen et al., 1997; Wang and Jacob, 1998; Tsigaridis et al., 2006; Naik et al., 2013a, b; Young et al., 2013; Murray et al., 2014; Khan et al., 2015).

When trying to get a better understanding of the response of clouds to aerosol perturbations, or when comparing this effect between models, the choice of oxidant level may not be important as long as there is consistency between the different models. However, the oxidant level may be important when the ~~modelled~~-modeled preindustrial-to-present-day total aerosol indirect effect is used as an estimate of the contribution from aerosol-cloud interactions to the total forcing of climate change since PI, as was done in IPCC AR5. Recent global model estimates of the aerosol indirect effects do, to a larger extent than before, represent more of the gas to aerosol formation processes through oxidation followed by nucleation (Boucher et al., 2013; Lohmann, 2017), increasing the importance of understanding the effects and the model treatment of the oxidants. More and more models will also incorporate an interactive atmospheric gas phase chemistry in transient climate studies, making the characterisation of effective radiative forcing a larger challenge. With this study we aim to use model simulations to investigate the impact on aerosol indirect effects from historical oxidants changes by letting the aerosol precursor gases in the PI-simulation be exposed to PI- instead of PD-oxidant ~~levels~~level.

Information about the model and the configurations applied in this study is found in Sect. 2. The experimental setup for the default model configuration and the experimental setups where the impact of separate oxidant changes is found in Sect. 3. In Sect. 4, the results are presented and discussed, divided into subsections focusing on the effect of the oxidant changes on the aerosol number concentration (Sect. 4.1.1), on the cloud droplet number concentration (Sect. 4.1.2) and on the aerosol indirect effect (Sect. 4.1.3). The results and discussions of the sensitivity tests where the oxidant changes were separated are found in Sect. 4.2, while six other sensitivity tests are studied in Sect. 4.3.

2 Model

2.1 General description

The model used in this study is CAM5.3-Oslo (Kirkevåg et al., 2018), which is an updated version of the atmospheric component of the Norwegian Earth System Model (NorESM) (Bentsen et al., 2013; Iversen et al., 2013; Kirkevåg et al., 2013). CAM5.3-Oslo is based on the Community Atmospheric Model version 5.3 (Neale et al., 2012; Liu et al., 2016), but has its own aerosol module (OsloAero). It also includes other modifications, such as the implementation of heterogeneous ice nucleation (Wang et al., 2014; Hoose et al., 2010). OsloAero has 21 aerosol tracers, distributed among six species (~~su~~lphate~~sulfate~~ (SO₄), secondary organic ~~aerosols~~-aerosol (SOA), black carbon, organic matter, mineral dust and sea-salt), ~~and~~ four precursor gases (SO₂, dimethyl sulfide (DMS), isoprene and monoterpene), three condensable gases (sulfuric acid (H₂SO₄), SOA_{LV} and SOA_{SV}) and H₂O₂. DMS-emissions are wind-driven and based on Nightingale et al. (2000), emissions of SO₂ are interpolated from a prescribed monthly mean decadal climatology given by Lamarque et al. (2010). The emissions of SO₂ in CAM5.3-Oslo deviates from Lamarque et al. (2010) when it comes to aircraft emissions and volcanic emissions, where the former is not included in CAM5.3-Oslo and the latter is included in the model but not in Lamarque et al. (2010). The emissions of the Biogenic Volatile Organic Compounds (BVOCs) isoprene and monoterpene are calculated online every timestep of half an hour by a satellite phenology version of the Community Land Model version CLM4.5 (Oleson et al., 2013), using the Model of Emissions of Gases and Aerosols from Nature version 2.1 (MEGAN2.1) (Guenther et al., 2012), where the emissions are impacted by both radiation and temperature, inducing a diurnal variation. An overview of global emissions and burdens of the precursor gases in CAM5.3-Oslo is found in Table 1. The aerosol nucleation is based on Makkonen et al. (2014), with improvements described in Kirkevåg et al. (2018), ~~which includes nucleation of both~~. This nucleation scheme is divided into two parts, where the binary homogeneous sulfuric acid-water nucleation based on Vehkamäki et al. (2002) can act in the whole atmosphere, while the activation type nucleation of H₂SO₄ and SOAorganic vapor based on Eq. (19) in Paasonen et al. (2010) occurs only in the boundary layer. The survival rate of particles with diameter from 2 nm to 23.6 nm (where the upper limit corresponds to the smallest sized particles that are accounted for in the aerosol number concentration in the model) follows Lehtinen et al. (2007). The stratiform clouds are ~~treated~~-described by the two-moment bulk microphysics scheme ~~MG1.5~~, that is almost identical to MG1 described in Morrison and Gettelman (2008), but with cloud droplet activation moved before the cloud microphysical process rates calculations (Gettelman, 2015; Gettelman and Morrison, 2015).

Methods by Ghan (2013) are used for calculating the effective radiative forcing of aerosols. The part called "cloud radiative forcing", or ΔC_{clean} is often used as a measure of ~~aerosol indirect effects~~the total aerosol indirect effect, where it represents the difference in the top of the atmosphere total cloud forcing between simulations performed with different aerosols. The "clean"-subscript indicates that the cloud forcing is based on separate calls to the radiation code where the scattering and absorption of radiation by the aerosols in the air around the cloud is neglected. ΔC_{clean} also includes semi-direct effects, but additional simulations with CAM5.3-Oslo with non-absorptive aerosols have shown that this term is negligible compared to the indirect effects in the model global mean PD-PI values (Kirkevåg et al., 2018). Henceforth we use ΔC_{clean} as a measure of ~~aerosol indirect effects~~the total aerosol indirect effect in this study.

2.2 Oxidant chemistry

CAM5.3-Oslo includes simple chemistry for sulfur and SOA species, which makes use of the chemical preprocessor MOZART (Emmons et al., 2010) modified for the CAM framework (Liu et al., 2012). The preprocessor is a numerical scheme that generates code to the model based on some input chemical reactions and rates. The generated code provides information of how the chemical tracers evolve as a function of concentration of chemical species. Reactions (R1-R10) in Table ??-2 represent the gas phase oxidation of the precursor gases in the model. SOA_{LV} and SOA_{SV} are both gaseous SOA (SOA(g)), low volatile and semi-volatile respectively, where only 50 % of the former can take part in nucleation, while both can condense on already existing aerosols. While (R2) represents the H abstraction part of the complex reaction where DMS is oxidized by OH, (R3) represents the OH addition part. At standard conditions (temperature of 273.13 K and pressure of ~~1.013~~ 10^5 1013 hPa), the ratio between the reaction rates of (R2) and (R3) is 7/13 (R2/R3). Methanesulfonic acid (MSA) is produced in (R3) following Chin et al. (1996). Since CAM5.3-Oslo does not trace MSA, ~~the product is put in the SOA-tracers, since MSA can contribute to aerosol~~ 20 % of the MSA is put into the SOA_{LV}-tracer, while 80 % is put into the SOA_{SV}-tracer. The exact yields are unknown, but there are studies supporting that MSA can obtain low enough volatility to contribute to new particle formation and growth (Berk et al., 2014)(Bork et al., 2014; Willis et al., 2016; Chen and Finlayson-Pitts, 2017). The oxidation of ~~biogenic-volatile organic compounds (BVOC)~~ BVOCs in (R5-R10) are based on Makkonen et al. (2014), but with some extensions explained by Kirkevåg et al. (2018). The yield of 15 % for monoterpenes (considered to be α -pinene in this model) is widely used in other global models (Dentener et al., 2006; Tsigaridis et al., 2014). The yield for isoprene varies more between different laboratory and model based studies (0.9–12 %) (Lee et al., 2006; Kroll et al., 2005; Spracklen et al., 2011; Jokinen et al., 2015), where the yield applied in CAM5.3-Oslo of 5 % is within this range.

The model also includes aqueous phase oxidation of SO₂ by H₂O₂ and O₃ (Tie et al., 2001; Neale et al., 2012). H₂O₂ production and loss are calculated online through reactions (R11-R13) in Table ??-2.

The concentrations of the other oxidants (NO₃, O₃, OH and HO₂) are prescribed by ~~interpolated~~ monthly mean values produced by ~~a global model with full chemistry (Lamarque et al., 2010)~~ the global full chemistry model CAM-chem v3.5 in the study of Lamarque et al. (2010). PD and ~~PI-values~~ PI-values used in this study are taken from decadal climatologies around year 2000 and 1855 respectively, and the percent change in the annual mean values can be seen in Fig. ??-1. NO₃ experiences a very large ~~relative~~ change between PI and PD (up to more than 1000 % in the northern hemisphere), which is also seen in other model studies (~~Khan et al., 2015)~~ that show good agreement between modeled present-day concentrations of NO₃ and observations (Khan et al., 2015). The prescribed PI-values of surface layer O₃ in the region around Paris used in this study are around a factor two higher than the measured PI-values at a station near Paris in the study of Volz and Kley (1988) (\sim 10 ppb). This overestimation of the PI-level of O₃ compared to observations corresponds with finding from other studies (Parrish et al., 2014). Evaluation of present-day concentrations of OH in a comparable version of CAM-chem shows reasonable agreement with the Spivakovsky et al. (2000) climatology (Lamarque et al., 2012). Simulated tropospheric concentrations of O₃ also agree well with ozone sondes, except for an overestimation over Eastern US and Europe (Lamarque et al., 2012; Brown-Steiner et al., 2018).

CAM5.3-Oslo ~~also~~ applies a daily cycle to OH and HO₂, which is not included in CAM5.3. ~~The prescribed oxidants in Fig. ?? are only applied in the chemistry of the model, and not for radiation calculations. O₃ is also important for radiation calculations, but here another prescribed O₃ field is applied, which~~ One should also be aware that the ozone climatology used for the radiation in the model is different from the ozone climatology used for the chemistry (the ozone climatology for radiation is the same in both PI and PD the PI- and PD-simulations).

2.3 Configurations

The model was configured with a horizontal resolution of 0.9° (latitude) by 1.25° (longitude) and 30 hybrid levels between the surface and ~3 hPa. The simulations were carried out using nudged meteorology produced by the model itself to constrain the natural variability (Kooperman et al., 2012). The horizontal wind components (U, V) were nudged with a relaxation time scale of six hours, while the temperature was ~~allowed to run free, enabling evolving free, allowing~~ impacts by aerosol perturbations, which could be important when calculating indirect effects (Zhang et al., 2014). Prescribed climatological ~~SSTs~~ sea surface temperatures and sea-ice extent from the mean of 1982-2001 were used in all simulations, as well as greenhouse ~~gases~~ gas concentrations and land use information from year 2000.

3 Experimental setup

3.1 General

Figure ~~?? shows an overview of~~ 2 describes how the simulations were carried out. The model was first run for six years to ~~output generate~~ instantaneous meteorological data. ~~This simulation used using~~ PD-conditions for ~~all possible choices~~ emissions, prescribed oxidant, and all other boundary conditions. All other simulations were nudged to the meteorology of this simulation. For each modification to the default model setup, three different simulations were carried out. These three simulations used the prescribed precursor- and aerosol emissions and oxidant concentrations given in Table ~~??~~ 3. Each of them was restarted from an ~~earlier simulation that was~~ already spun up ~~ease with~~ for two years with free meteorology, applying emissions and oxidants from ~~its the same~~ era. The ~~nudged simulations where then run for four years, where the last three years of the simulations were analyzed~~ were analyzed. Sensitivity tests with CAM5.3-Oslo (not shown here) show that ~~analyzing only these three years gives a standard error due to natural variability of only 0.01 Wm⁻² for the total aerosol indirect effect, and a magnitude of the total aerosol indirect effect that is the same as when running the nudged simulations for 11 years and analyzing the last ten years.~~ To lower the computational cost, the simulations in this study apply the setup described above, except for one sensitivity test in Sect. 4.3 where longer simulations with free meteorology are examined. The first set of simulations used CAM5.3-Oslo as described ~~above in the previous section~~, without any other modifications to the code. We name these simulations ORG, and the impact of historical oxidant changes on the PD-PI ~~indirect effects~~ total aerosol indirect effect in CAM5.3-Oslo are quantified by the difference we ~~get obtain~~ (relative to the PD simulation PDAER_PDOXI_ORG) when switching between the two PI-simulations PIAER_PDOXI_ORG and PIAER_PIOXI_ORG.

3.2 Decomposing the oxidant change

To estimate the importance of the different changes in the individual oxidants between PI and PD, four additional simulations with PI-aerosols were carried out. In these simulations, the oxidant of interest was changed to PI-concentrations, while all other oxidants were kept at PD-levels. Acknowledging the complexity of oxidant chemistry, one can not expect that separate oxidant changes in separate simulations will add up to the same result as changing them all simultaneously. To explore the importance of this non-linearity, another four additional simulations were performed, keeping all oxidants from PI except for the one of interest, which was set to PD-levels.

4 Results and discussion

4.1 Original setup

10 The top panels of Fig. [??-3](#) show the PD-PI indirect effect for ~~shortwave radiation~~ (a) ~~longwave radiation~~[shortwave radiation](#),
(b) ~~and total radiation~~[longwave radiation](#), and (c) [total radiation](#) when using the standard setup with PD-oxidants in both simulations. The bottom panels of Fig. [??-3](#) show the impact of historical oxidant changes on the PD-PI indirect effect. Figure [??-3](#)(d) shows that letting the precursor gases in the PI-simulation be exposed to oxidants from its era, instead of oxidants from PD, makes the shortwave indirect effect 0.39 Wm^{-2} less negative (changing from -1.48 Wm^{-2} to -1.09 Wm^{-2}). This implies
15 that the clouds in the PI-simulation with PI-oxidants are cooling the climate more through SW-effects than the clouds in the PI-simulation with PD-oxidants, reducing the difference in shortwave cloud forcing between PI and PD. Figure [??-3](#)(e) shows that the change in longwave indirect effect is -0.14 Wm^{-2} (from 0.16 Wm^{-2} to 0.02 Wm^{-2}), meaning that the clouds in the PI-simulation with PI-oxidants are warming the climate more through increased absorption of longwave radiation, reducing the difference in longwave cloud forcing between PI and PD. Figure [??-3](#)(f) shows a total (shortwave + longwave) change in
20 the indirect effects of $+0.25 \text{ Wm}^{-2}$ (changing from -1.32 Wm^{-2} to -1.07 Wm^{-2}), meaning that the PI-clouds with PI-oxidants are cooling the climate more than the PI-clouds with PD-oxidants, thus making the indirect effect less negative. The largest changes in the shortwave indirect effect occur over ocean, especially over the North Pacific, off the west coast of America, in remote areas between 30° S and 60° S and over the Indian Ocean. The changes in the longwave indirect effect mainly take place in the polar regions and over the Indian Ocean.

25 Different cloud- and aerosol changes can help explain the resulting change in the indirect effect. Some of these are presented in Fig. [??-4](#). In the global mean, switching to PI-oxidants in the PI-simulation results in (a) more numerous aerosol particles (+9.2 %), (b) more numerous cloud droplets (CDNC) (+3.7 %), (c) smaller cloud droplets (-1.5 %), (d) larger cloud fraction (+0.26 %), which is mainly caused by changes in the low cloud fraction, and (e) larger total gridbox averaged liquid water path (LWP) (+1.7 %). The size of the cloud droplets in Fig. [??-4](#)(c) is taken from the cloud top layer of the stratiform clouds.

30 The sign of the changes in the global mean cloud and radiative properties seen in Figs. [??-and-??-3](#) and [4](#) is as expected for an increase in the global mean aerosol number concentration. We will now further investigate why the oxidant changes enhance the aerosol number concentration. Figures [??-and-??-3](#) and [4](#) show that the distribution of the changes in aerosol number

concentration does not always correspond directly to the distribution of the changes in the cloud and radiative properties. This indicates that it is not only the change in aerosol number concentration that is important for the result, but also changes in the composition of the aerosols and in the atmospheric conditions where the aerosol changes take place.

4.1.1 The increase in aerosol number concentration

5 Since the formation of new aerosols depends on the availability of ~~low-volatile~~low-volatility gases, and the PI-atmosphere consisted of relatively small amounts of oxidants to produce secondary gases with reduced volatility, one could expect a reduction in the aerosol number concentration when switching from PD- to PI-oxidants. This is the opposite of what Fig. ~~??4~~(a) shows. The increased lifetime of the precursor gases and the aerosols seen in Table ~~??~~partly explain ~~4~~partly explains this. When the oxidizing power of the atmosphere is reduced, the precursor gases with high volatility are transported higher up in the atmosphere before they are oxidized. This is seen in Fig. ~~??5~~, where the relative change in chemical loss of (a) DMS, (b) SO₂, (c) isoprene, and (d) monoterpene through oxidation is negative close to the surface, but positive higher up in the atmosphere when switching from PD- to PI-oxidants in the PI-simulation. This ~~results in~~pattern corresponds well with the change in the vertical profile of the aerosol number concentration seen in Fig. ~~??9~~(a), with lower values close to the ~~ground~~surface, but larger values above ~900 hPa. Aerosols formed from gases higher up in the atmosphere are not removed
15 by ~~dry- and wet-deposition~~deposition as easily as aerosols formed closer to the ~~ground, explaining the longer aerosol lifetime seen in Table ??~~surface (Jaenicke, 1980; Williams et al., 2002). ~~This is seen in the results of this study where the dry deposition of the newly formed nucleation mode SO₄ and SOA decreases by 2.6 %. The wet deposition stays the same. This total decrease in deposition is one of the factors contributing to the increase in the aerosol number concentration seen in Fig. 4(a).~~

20 It is not only the vertical transport of the gases that changes. The reduced oxidation capacity also increases the horizontal transport of the primary precursors away from the source regions. This is, e.g., seen in Fig. ~~??, focusing on 6~~ for DMS, the main precursor gas over ocean, where most of the aerosol-, cloud- and radiation changes occur. Figure ~~??6~~(a) shows the distribution of DMS-emissions, which is equal in all PI-simulations, while Fig. ~~??6~~(b) shows the change in the ~~net~~-chemical loss of DMS through oxidation when switching from PD- to PI-oxidants. Increased horizontal transport happens from areas
25 with negative values to areas with positive values, since chemical loss through oxidation is the only way DMS can be lost in the model. The increase is especially pronounced in the North Pacific, with increased transport further south and towards the Arctic, but is also found in the southern ~~oceans~~ocean with increased transport from the large emission sources close to the coast ~~and~~-towards the remote ocean. Figure ~~??6~~(c) shows that this transport results in increased aerosol formation close to the ~~ground~~surface in areas that receive more DMS with PI-oxidants. Since the precursor gases are spread more in space
30 with PI-oxidants, towards more remote areas where the background concentration of aerosols are low, the coagulation sink during the nucleation process is reduced, contributing to an increase in the formation rate. In CAM5.3-Oslo, "formation rate" describes the formation of aerosol particles ~~of 12~~with diameters of 23.6 nm, which is the size limit a particle must achieve to be accounted for in the aerosol number concentration (Figs. ~~??4~~(a) and ~~??6~~(e)). "Nucleation rate" ~~describe~~describes the formation of aerosol particles with diameters of 2 nm. As for all ~~other~~-aerosols, the particles between 2 and ~~12 nm can also~~23.6

nm can be lost through coagulation with background aerosols. Figure ??6(d) shows how the coagulation sink of these particles changes when switching from PD- to PI-oxidants in the PI-simulation. The reduction in the coagulation sink is especially large close to the strong DMS-emissions sources (Fig. ??6(d)). The areas over ocean with increased formation rate close to the ground-corresponds-surface correspond well with the areas in Fig. ??6(e) with increased aerosol number concentrations, indicating that the horizontal transport of DMS due to its longer lifetime in an atmosphere with PI-oxidants is important for the increase in aerosol number concentration. Higher up in the atmosphere (above ~ 850 hPa), the formation rate of aerosols also increase-increases over the emission sources and at higher latitudes (not shown). The change in the total vertically integrated coagulation sink decreases by 17.7 % when switching-switching from PD- to PI-oxidants in the PI-simulation, favouring-favoring enhanced formation of new aerosols. Increased-As the lifetime of the precursor gases also-results-in-an-increased-and the cloud amount increases, the total deposition rate of SO_2 of-12.8-increases with 7.4 % (DMS, isoprene and monoterpene are only lost through atmospheric chemistry), favouring-favoring a decrease in the formation of new aerosols. As a result of these-two-all the competing effects, the total vertically integrated formation of new aerosols increases by 5.4 %.

Some of the newly formed SO_4 and SOA are lost through coagulation with the background aerosols. This coagulation sink is also reduced (-3.6 %) when switching from PD- to PI-oxidants for the same reasons as for the particles between 2 and 23.6 nm, contributing to the change in the aerosol number concentration seen in Fig. 4(a).

Even though Fig. 6 shows that the increased lifetime of the precursor gases partly can explain why the aerosol number concentration increases when switching from PD- to PI-oxidants, other factors could also play a role. The precursor gases have the potential of being oxidized in three different ways, resulting in different amounts of the end products H_2SO_4 , SOA_{LV} and SOA_{SV} . While both H_2SO_4 and SOA_{LV} can take part in nucleation (to nucleation mode SO_4 and nucleation mode SOA, respectively), SOA_{SV} can only condense onto already existing particles. If changes in the oxidation pathways favor more production of H_2SO_4 or SOA_{LV} , it can contribute to the increase in the aerosol number concentration seen in Fig. 4(a). The left panels of Fig. 7 show the contribution of the different reactions to the oxidation of the precursor gases. The largest change in the oxidant level when switching from PD- to PI-oxidants is found for NO_3 in the northern hemisphere (Fig. 1(c)). When switching to PI-oxidants, the relative fraction of DMS, isoprene and monoterpene oxidized by NO_3 is reduced (Fig. 7(a,c,d), red curves), while the oxidation involving the other oxidants become more important. For DMS, Fig. 7(a) shows that this change in the oxidation pathway will reduce the formation of species that can take part in nucleation since some of it will be converted to SOA_{SV} instead of SO_2 (that later becomes H_2SO_4). For monoterpene, switching to PI-oxidants favors an oxidation pathway that gives more SOA_{LV} (Fig. 7(d)), thus favoring an increase in the aerosol number concentration. An overview of all the conversion rates for the oxidation reactions in the two simulations with different oxidants is found in Table 5. Even though the global burden of nucleation mode SO_4 -aerosols increases (+0.00650 Tg, +8.8 %), Table 5 shows that the production of H_2SO_4 decreases when switching from PD- to PI-oxidants (-0.5 Tg yr^{-1}), indicating that a shift towards more production of H_2SO_4 that can nucleate is not an explanation for the increase in the aerosol number concentration seen in Figure 4(a). The global burden of nucleation mode SOA-aerosols is also increasing (+0.00450 Tg, +12 %). Contrary to the case of SO_4 , Table 5 shows that this could partly be due to a shift towards more production of a gas that can take part in nucleation since the

production of SOA_{LY} increases ($+1.63 \text{ Tg yr}^{-1}$). Sensitivity tests in Sect. 4.3 will show that this increase in production of SOA_{LY} has a negligible impact on the results in this study.

4.1.2 The increase in cloud droplet number concentration

Figure ?? Figure 4(b) shows that the CDNC increases in regions that experience large relative changes in the aerosol number concentration (Fig. ??4(a)). The aerosol number concentration and CDNC increases are linked to the extended DMS lifetime discussed above (Fig. ??6(b)), which in turn allows for more DMS transport to and subsequently increased aerosol formation in remote regions like the South Pacific (SP) and the Arctic Ocean (AO), as defined in Fig. ??8. The region named North Pacific (NP) in Fig. ??8 experiences a local minimum in the change in the aerosol number concentration. Figure ??6 shows that this is caused by less aerosol formation in this region. Nevertheless, NP also experiences a relatively large increase in CDNC. The vertical profiles in Fig. ??9 show that the regions which receive more precursor gases with PI-oxidants (AO and SP) experience an increase in both aerosol number concentration and CDNC for all altitudes, while the NP region experiences a decrease close to the ground surface, but an increase higher up aloft. The latter can be explained by the vertical shift in the oxidation (Fig. ??5). In NP, the height above which the change in CDNC is positive is located lower down in the atmosphere than the height at which the aerosol number concentration starts to increase (Fig. ??Figs. 9(i) and ??9(l)). This can be explained by the change in the size of the aerosols (Fig. ??9(j)), caused by the increased aerosol condensate relative to the aerosol number concentration (Fig. ??9(k)). The mean size of the aerosols is calculated as a mean of the number mean radius of all mixtures in the model, weighted by the number of aerosols in each mixture. The relative amount of condensate increases in the global mean (Fig. ??9(c)) and in the northern hemisphere (Fig. ??9(g) and ??9(k)) because of the strong shift in the importance of the different oxidation reactions (Fig. ??). Both DMS, isoprene, monoterpene and SO_2 have the potential of being oxidized in three different ways. Figure ?? shows how many percent of the oxidant reactions of a specie happening through the different reactions. The largest change in the oxidant level when switching from PD to PI-oxidants is found for NO_3 in the northern hemisphere (Fig. ??(e)). When switching to PI-oxidants, the relative fraction of DMS oxidized by NO_3 is reduced (Fig. ??(a,c,d), red curves), while the the oxidation fraction involving the other oxidants become more important. For 7). This means for DMS, the dominant precursor gas over the remote oceans, DMS, this means that instead of mostly getting $1 \cdot \text{SO}_2$ and no SOA out off a DMS-oxidation through the reaction from an oxidation of DMS through (R4), the PI-atmosphere will to a larger extent produce $0.75 \cdot \text{SO}_2$ and some SOA through (R3). SO After SO_2 has been oxidized to H_2SO_4 , it nucleates easier than SOA, and 80 % of the SOA from (R3) comes as SOA_{SV} , which is only allowed to condense. The change in aerosol size in SP (Fig. ??9(n)) deviates from the other regions. This is due to the increase in OH in SP when switching to PI-oxidants (blue colors in Fig. ??1(a)), giving rise to enhanced nucleation of small SO_4 -aerosols followed by an enhanced H_2SO_4 -production through (R1). This also happens in AO, where the OH-level also is larger in PI, but here this effect is small relative to the effect of the increased SOA_{SV} -production due to the large NO_3 -change in the northern hemisphere (Fig. ??1(c)).

4.1.3 The change in aerosol indirect effect

The SW radiative effect of a change in CDNC varies depending on where these changes take place. Twomey (1991) showed that $dA/d(\text{CDNC})$, where A is the cloud albedo, is largest in clean regions with low CDNC and where the cloud albedo is approximately 0.5. The SW radiative effect will also be larger in areas with low surface albedo, in areas close to the equator due to more incoming solar radiation, and in areas where the cloud fraction is high. The last two factors, in addition to the factors in Twomey (1991), are taken into account in Eq. (6) in Alterskjær et al. (2012) when finding a cloud-weighted susceptibility function. This is a hybrid between the simplified $dA/d(\text{CDNC})$ of Twomey and the more complex $d(\text{ERFaci})/d(\text{CDNC})$, which we see in Figure ???. It only includes the first aerosol indirect effect, and not second aerosol indirect effects (such as increased lifetime, cloud amount and cloud extent). The susceptibility function ~~will give~~ gives an indication of which areas over ocean ~~being that are~~ relatively more susceptible than others to cloud albedo changes caused by changes in CDNC. The cloud-weighted susceptibility function is normalized by its maximum value. Applying this function to three years of daily output from the PIAER_PDOXI_ORG-simulation in this study results in Fig. ??10(a). Areas with high cloud-weighted susceptibility are found off the west coast of the continents and in the remote southern ocean storm tracks. The large increase in CDNC (Fig. ??4(b)) in the North and South Pacific regions efficiently ~~increase~~ increases the albedo of the clouds, thus resulting in the large change in the SW indirect effect seen in Fig. ??3(d). Due to less insolation in the Arctic, the cloud-weighted susceptibility in this region is low, resulting in a negligible effect on the SW indirect effect, even though this is the region that experiences the relatively largest increase in both CDNC (Fig. ??4(b)), cloud fraction (Fig. ??4(d)) and LWP (Fig. ??4(e)) due to the oxidant changes. The LW indirect effect is not dependent on the incoming solar radiation, so the large changes in cloud properties seen in the Arctic affect the LW indirect effect. The thicker and longer-lived clouds in the simulation with PI-oxidants act to reduce the difference in LW heating between the PD- and PI-simulations (Fig. ??3(e)). Figure ??10(b) shows the vertical profile of the global mean cloud-weighted susceptibility. It shows that the decrease in CDNC close to the ~~ground surface~~ (Fig. ??9(d)) does not affect the cloud albedo as much as the increase in CDNC between 900 and 800 hPa.

4.2 Decomposing the oxidant change

To get a better understanding of the results in the original experiment, results from the sensitivity tests where only one oxidant at a time was changed are analyzed. Figure ??-11 shows differences in the global mean shortwave and longwave indirect effect between the setups with modified PI-simulations (PIOXI, PIOH, PIO3, PINO3 and PIHO2) and the original setup with only PD-oxidants in both simulations. Figure ??-12 shows the same for the horizontal distribution. Changing only NO_3 (PINO3) gives almost the same result as changing all of the oxidants (PIOXI), indicating that the historical change in NO_3 is the most important oxidant change for indirect effect calculations. This corresponds well with Fig. ??-1 showing that NO_3 is the oxidant that has experienced the largest relative change since PI, and Fig. ??-7 showing that the importance of the oxidation reactions involving NO_3 ~~drop~~ drops the most when switching from PD- to PI-oxidants in the PI-simulation. The negative pattern over land in the tropics in PINO3 that is missing in PIOXI (Fig. ??12) seems to be explained by the changes in O_3 . Analysis of the PIO3-simulation shows that replacing only the O_3 -oxidant with PI-values reduces the importance of (R6) where monoterpene is

oxidized by O_3 giving SOA_{LV} , while the other oxidation reactions of monoterpene giving SOA_{SV} become more important. This results in less new aerosol formation and increased growth of the already existing aerosols through condensation, increasing the CCN-concentration and the following cloud droplet activation and CDNC.

Table ??-6 shows that there are some non-linearities associated with changing one oxidant at a time. The odd numbered rows show the impact on the indirect effects when changing one oxidant at a time, while the even rows show the difference in the effect of changing all oxidant and changing all except for one oxidant. If there were no non-linearities involved in the oxidant chemistry, ~~a-an~~ odd numbered row and the following row would have shown the same numbers. This is not the case, but the differences are relatively small, supporting the indication that the contributions to the total result mainly stem from the historical changes in NO_3 .

10 4.3 Sensitivity tests

Due to nonlinear processes and feedbacks in the model, it is difficult to separate the different effects and to estimate how much each of them contributes to the final result. As an example, enhanced formation of new aerosols can be explained as in Sect. 4.1.1, starting by the increase in lifetime of the precursor gases, but the enhanced importance of reactions giving SOA ~~suffieiently with~~ with sufficiently low volatility to nucleate new aerosols ((R3) and (R6)) can also be a part of the explanation. To get a better understanding of the importance of the various factors and processes, extra sensitivity tests with ~~four-six~~ new setups were carried out, ~~all of them consisting-~~ All the test consists of three different simulations, as illustrated in Fig. ??, ~~all deviating-2~~. They all deviate from the original set-up-setup as well as from Kirkevåg et al. (2018), either through changes in some of the chemical reactions (R1-R10), ~~or directly through~~ manipulating the aerosol input to the code for cloud droplet activation, manipulating the code that treats the oxidants or changing the constraint on the meteorology. Information about the ~~setup-setups~~ for the sensitivity tests ~~are-is~~ found in Table ??7.

4.3.1 NOSOALVDMS and NOSOALVBVOC

When moving from a high NO_3 -regime (PD-oxidants) to a low NO_3 -regime (PI-oxidants), the oxidation reactions giving SOA_{LV} as a product ((R3) and (R6)) become more important. This is seen from the large change in the global mean column burden of SOA_{LV} (+49.6 %). Since SOA_{LV} can take part in nucleation and can give rise to the increased aerosol number concentration seen in Fig. ??4(a), the additional SOA_{LV} that is produced when using PI-oxidants may explain the change in the indirect effects seen in Fig. ??3. When replacing all of the ~~originally standard~~ produced SOA_{LV} from the DMS-oxidation in (R3) with SOA_{SV} in the NOSOALVDMS-simulations, the change in the total aerosol indirect ~~effects-effect~~ is almost the same as for the original setup (ΔAIE_{tot} : $+0.25 \text{ Wm}^{-2}$), and the geographical pattern looks largely the same (not shown here). This also holds when doing the same for the oxidation of monoterpene (R6) (ΔAIE_{tot} : $+0.26 \text{ Wm}^{-2}$). The pattern of the resulting AIE from the oxidant changes in the NOSOALVBVOC-simulations looks almost the same as for the original simulations, except over the Amazon where the signal from the O_3 -changes explained in the last section is gone. This does not change the global mean AIE by more than 0.01 Wm^{-2} , however. These sensitivity tests indicate that even though the global mean burden of SOA_{LV} changes a lot when using PI-oxidants, this plays a minor role for the change in the indirect effects seen in Fig. ??3.

4.3.2 NOSOA

The increased production of total SOA(g) (SOA_{SV} and SOA_{LV}) when switching from PD to PI-oxidants has the potential to cause changes in the indirect effects even though the nucleation effect is negligible. All SOA(g) can condense onto already nucleated aerosols and make it easier for them to grow to the critical size for cloud droplet activation, except for cases where
5 the reduction in hygroscopicity is more important than the increase in size. The impact of the hygroscopicity changes due to the changes in the oxidant levels has been tested and found to be negligible (not shown here). The change in total global mean column burden of SOA(g) due to changes in the oxidant ~~levels~~ level with the original setup was +40.7 %. To find out if whether this increase is causing the change in the indirect effects seen in Fig. ??3, the model was run with the NOSOA-setup described in Table ??7. This resulted in a change in the total aerosol indirect effects (ΔAIE_{tot}) of $+0.14 \text{ Wm}^{-2}$, deviating by more
10 than 0.10 Wm^{-2} from the original setup. Removing products from the reaction makes the atmosphere cleaner, thus creating a different regime ~~for both~~ both for aerosol growth through reduced competition for condensable gases ~~and for activation of aerosols~~ as for aerosol activation through reduced competition for water ~~vapor~~ vapour. This means that one cannot conclude that 0.11 Wm^{-2} of the 0.25 Wm^{-2} is caused by an increase in condensable SOA(g) when switching from PD- to PI-oxidants, but this sensitivity test indicates that it may have contributed to the overall result seen in Fig. ??3.

15 4.3.3 NACTOFF

This test is performed in order to see how important the change in the droplet activation on the smallest aerosols ~~are~~ is. When modifying the oxidant level, the smallest aerosols are affected by the change in formation rate, while all aerosols are affected by the change in condensation. The results from this test give an indication of how important the changes associated with the smallest aerosols are. When not allowing the smallest aerosols in mixture number 1 (corresponding to the nucleation
20 mode in modal aerosol schemes) to activate, the change in the total aerosol indirect effects found when switching from PD- to PI-oxidants in the PI-simulation is small (ΔAIE_{tot} : -0.03 Wm^{-2}). This confirms that it is the difference in the number concentration of the smallest SO_4 - and SOA-aerosols between the simulations with different oxidant levels that gives the large difference in the indirect effect seen in Fig. ??3.

4.3.4 DIURNALNO3

25 The tests where the oxidant changes were studied individually identified the historical change in NO_3 as having the largest impact on the result. As described in the model description, OH and HO_2 have a diurnal cycle added to the prescribed monthly climatology in CAM5.3-Oslo. This is not the case for NO_3 , even though it is well known that concentrations of NO_3 drop during daytime due to rapid photolysis (Wayne et al., 1991; Seinfeld and Pandis, 2016). To see how this lack of a diurnal cycle for NO_3 impacts the results in this study, another set of simulations was carried out. The daytime concentration of NO_3 was set
30 to zero, while the nighttime concentration was increased, such that the daily averaged and the monthly averaged values stayed the same as in the original setup. This treatment of the diurnal cycle is the same as that for HO_2 and OH, but with a shift from day to night. Carrying out the same three model simulations with this new setup as for the original default model setup gives

a change in the total aerosol indirect effect of $+0.26 \text{ Wm}^{-2}$ (from -1.32 Wm^{-2} to -1.06 Wm^{-2}) when applying PI- instead of PD-oxidants. In other words, this test shows that the lack of a diurnal cycle for NO_3 only has a minor influence on the result in this study. The reason for this minor impact is that the main effect of oxidation by NO_3 is of DMS over the oceans. Since the lifetime of DMS is 36 and 55 hours (present-day and preindustrial respectively), the reduction in the nighttime oxidation when not applying a diurnal cycle will have time to be compensated by an increase in the daytime oxidation.

4.3.5 FREEMET

Constraining the natural variability by nudging the meteorology has been shown to be an efficient way of identifying the effect of a model perturbation since it reduces the computational cost and time significantly (Kooperman et al., 2012). In this study, nudging has been applied in order to model ERF_{aci} . According to the definition of effective radiative forcing in Myhre et al. (2013, p. 665), "ERF represents the change in net TOA downward radiative flux after allowing for atmospheric temperatures, water vapor and clouds to adjust, but with global mean surface temperature or a portion of surface conditions unchanged". In the simulations presented here, nudged winds are not fully impacted by rapid adjustments in the atmosphere due to an aerosol perturbation, which again could give a response by the clouds. Thus, parts of this rapid wind-aerosol-cloud-radiation feedback could be missing from the calculated values of ERF in this study. Running all the simulations in this study with free meteorology is computationally very expensive. Instead we performed sensitivity tests for the three simulations with the original model setup to estimate the bias introduced by the method of nudging. The length of the simulations is 53 years, where the last 50 are analyzed. The total aerosol indirect effect changes by $0.3 \pm 0.2 \text{ Wm}^{-2}$ (from $-1.3 \pm 0.2 \text{ Wm}^{-2}$ to $-1.0 \pm 0.2 \text{ Wm}^{-2}$) when switching from PD- to PI-oxidants in the PI-simulation. Even though the uncertainties due to natural variability still are large after 50 years, this change in the total aerosol indirect effect due to historical oxidant changes fall in the same range as when nudging the winds with a relaxation time scale of six hours. Analyzing only the last 30 years of the simulations gives the same change in the total aerosol indirect effect, indicating that there is no drift in the signal.

5 Summary and conclusions

~~Here we~~ We have used the global atmospheric model CAM5.3-Oslo to study the effect of historical oxidant changes on the PD-PI aerosol indirect effect. The precursor gases in the PI-simulation were exposed to PI-oxidants instead of PD-oxidants. Our main findings are:

- The total aerosol indirect effect is reduced from -1.32 Wm^{-2} to -1.07 Wm^{-2} , mainly due to a cloud brightening in the modified PI-simulation.
- NO_3 is the oxidant that contributes the most to the changes.
- When the precursor gases are exposed to an atmosphere with relatively lower oxidative power (PI-oxidants vs. PD-oxidants), their ~~lifetime increases~~ lifetimes increase and they are transported higher up in the atmosphere and horizontally towards more remote areas before they are oxidized ~~and can contribute to new aerosol formation.~~

– The increased lifetime of the precursor gases contributes to an increase in the formation of new aerosol and a decrease in the deposition and in the coagulation sink of the newly formed aerosols, contributing to an increase in the aerosol number concentration.

– A large portion of the new aerosol formation and the increase in aerosol number concentration occurs where the cloud-weighted susceptibility is high, giving a large impact on the radiative effects.

– The change from PD- to PI-oxidants in the PI-simulation yields a shift in the chemical reactions towards increased production of condensate relative to the amount of gases that can nucleate, which increases the size of the aerosols, making it easier for them to activate.

Note, that the magnitude of the sensitivity of the total aerosol indirect effect to the choice of the oxidants in this study is as large as the total sulfur direct forcing (Myhre et al., 2013), thus contributing significantly to the total preindustrial-to-present-day anthropogenic forcing. Overviews of model results of the PD-PI aerosol indirect effect show occasionally so negative values that they even offset the warming from the greenhouse gases (Boucher et al., 2013; Lohmann, 2017). Our results suggest that such unrealistic cooling may appear less often if the precursor gases are exposed to oxidants of ~~its~~ their era, instead of applying PD-oxidants for both PD- and PI-simulations.

The results in this study are ~~only~~-based on simulations from just one model, with its model-specific treatments of oxidants, aerosols, clouds and radiation that all include uncertainties and simplifications. This also holds for the single input dataset used for the prescribed oxidants. An evaluation of the extent to which uncertainties in the different ~~schemes~~ parameterizations and in the prescribed oxidant fields affect the result is beyond the scope of this paper, but should be focus for future studies. The treatment of the MSA-product from DMS-oxidation by OH (R3) should be looked at in particular, since the changes in SOA-condensate from that reaction ~~seems seem~~ to contribute to the resulting changes in the total aerosol indirect ~~effect~~ effect. Different choices of yields for the oxidation reactions in Table 2 should also be in focus since these yields are uncertain and vary between different models and observations (Kroll et al., 2005; Lee et al., 2006; Dentener et al., 2006; Spracklen et al., 2011; Neale et al., 2012). The impact of the lack of pure biogenic new particle formation in the model applied in this study could also be studied, since this mechanism has been shown to be important for radiative forcing calculations, especially in clean regions (Gordon et al., 2016). When it comes to the oxidant input dataset, it would be interesting to see how the result is affected by using a model with online oxidant chemistry. Upcoming studies should also see how the result is affected by using other input datasets produced by more advanced models than the model applied in Lamarque et al. (2010), which for example did not include online aerosol-cloud radiative interactions or different land cover information in the two different eras, which could have impacted the oxidant level through different photolysis rates and different emissions from the land model.

The impact of the oxidant changes also ~~depend~~ depends on the emissions of precursor gases ~~in the model~~. Carslaw et al. (2013) show that there are large uncertainties linked to natural emissions, even when assuming that they do not vary between PI and PD. This was shown especially for DMS (Woodhouse et al., 2010), which is found to be one of the most important precursor gases in this study. Changes in temperature and pH in the ocean, as well as changes in land use, insolation, ~~CO₂~~ and more, and CO₂ may also have contributed to a change in the emissions since preindustrial time (Charlsson et al., 1987;

Guenther et al., 2012; Unger, 2014). CAM5.3-Oslo is also lacking some emissions that could be important for the magnitude of the effect of the oxidant changes, for example emissions of ~~biogenic volatile organic compounds (BVOCs)~~ BVOC from the ocean, which can contribute significantly to the marine aerosol loading (Shaw et al., 2010), creating a more polluted regime with the potential of different susceptibilities.

5 Despite the large uncertainties and simplifications mentioned above, we find that the treatment of the oxidants is open for discussion. We suggest that a common way of treating the oxidants must be agreed upon when modeling aerosol effective radiative forcings. We also encourage other researchers to specify which oxidants are used in their studies of historical changes in aerosol-cloud interactions.

Simulations from the Aerosol Chemistry Model Intercomparison Project (AerChemMIP), endorsed by the Coupled-Model
10 Intercomparison Project 6 (CMIP6) can be used to quantify preindustrial-to-present-day effective radiative forcings. Comparing the cloud forcings from the simulations called piClim-aer and piClim-control (Collins et al., 2017) will be approximately the same as done in the original default setup in this study, with the same oxidant level in both simulations. For models without tropospheric chemistry, AerChemMIP does not include a setup that takes into account historical oxidant changes. However, models that include tropospheric chemistry can perform the simulation piClim-NTCF, which includes different
15 ozone precursors in the two different simulations, giving a different oxidation capacity. The piClim-NTCF simulation does not include all the factors that contribute to the differences in the oxidant level between PD and PI (for example methane), but it includes some of them, so we suggest that a comparison of the cloud forcings in piClim-NTCF and piClim-control will facilitate calculations of the PD-PI aerosol indirect effect, including changes due to different oxidant ~~levels~~ level, also for the CMIP6-models.

20 *Competing interests.* The authors declare that they have no conflict of interest.

Acknowledgements. I. H. H. K., A. G., D. O., A. K., Ø. S., T. I. and M. S. have been financed by the research council of Norway (RCN) through the project EVA and the NOTUR/Norstore projects (Sigma2 account: nn2345k, Norstore account: NS2345K). We gratefully acknowledge Sara Marie Blichner and Moa Sporre for scientific discussions.

References

- Albrecht, B. A.: Aerosols, cloud microphysics, and fractional cloudiness., *Science*, 245, 1227–1230, <https://doi.org/10.1126/science.245.4923.1227>, 1989.
- 5 Alterskjær, K., Kristjánsson, J. E., and Seland, O.: Sensitivity to deliberate sea salt seeding of marine clouds - Observations and model simulations, *Atmospheric Chemistry and Physics*, 12, 2795–2807, <https://doi.org/10.5194/acp-12-2795-2012>, 2012.
- Bentsen, M., Bethke, I., Debernard, J. B., Iversen, T., Kirkevåg, A., Seland, Ø., Drange, H., Roelandt, C., Seierstad, I. a., Hoose, C., and Kristjánsson, J. E.: The Norwegian Earth System Model, NorESM1-M – Part 1: Description and basic evaluation, *Geoscientific Model Development Discussions*, 5, 2843–2931, <https://doi.org/10.5194/gmdd-5-2843-2012>, 2013.
- Berntsen, T. K., A Isaksen, I. S., Myhre, G., Fuglestedt, J. S., Stordal, F., Alsвик Larsen, T., Freckleton, R. S., and Shine, K. P.: Effects of anthropogenic emissions on tropospheric ozone and its radiative forcing, *Journal of Geophysical Research*, 102126, 101–28, <https://doi.org/10.1029/97JD02226>, 1997.
- 10 Bork, N., Elm, J., Olenius, T., and Vehkamäki, H.: Methane sulfonic acid-enhanced formation of molecular clusters of sulfuric acid and dimethyl amine, *Atmospheric Chemistry and Physics*, 14, 12 023–12 030, <https://doi.org/10.5194/acp-14-12023-2014>, 2014.
- Boucher, O., Randall, D., Artaxo, P., Bretherton, C., Feingold, G., Forster, P., Kerminen, V.-m., Kondo, Y., Liao, H., Lohmann, U., Rasch, P., Satheesh, S., Sherwood, S., Stevens, B., and Zhang, X.: Clouds and aerosols, in: *Climate Change 2013: The Physical Science Basis. Contribution of Working Group I to the Fifth Assessment Report of the Intergovernmental Panel on Climate Change*, edited by Stocker, T., D. Qin, G.-K., Plattner, M., Tignor, S., Allen, J., Boschung, A., Nauels, Y., Xia, V., Midgley, B., and P.M., chap. 8, pp. 659–740, Cambridge University Press, Cambridge, United Kingdom and New York, NY, USA., 2013.
- 15 Brown-Steiner, B., Selin, N. E., Prinn, R., Tilmes, S., Emmons, L., Lamarque, J.-f., and Cameron-smith, P.: Evaluating Simplified Chemical Mechanisms within CESM Version 1 . 2 CAM-chem (CAM4): MOZART-4 vs . Reduced Hydrocarbon vs . Super- Fast Chemistry, *Geoscientific Model Development Discussions*, pp. 1–40, 2018.
- 20 Carslaw, K. S., Lee, L. A., Reddington, C. L., Pringle, K. J., Rap, A., Forster, P. M., Mann, G. W., Spracklen, D. V., Woodhouse, M. T., Regayre, L. A., and Pierce, J. R.: Large contribution of natural aerosols to uncertainty in indirect forcing, *Nature*, 503, 67–71, <https://doi.org/10.1038/nature12674>, <http://dx.doi.org/10.1038/nature12674>, 2013.
- 25 Chameides, W. L., Fehsenfeld, F., Rodgers, M. O., Cardelino, C., Martinez, J., Parrish, D., Lonneman, W., Lawson, D. R., Rasmussen, R. A., Zimmerman, P., Greenberg, J., Mlddleton, P., and Wang, T.: Ozone precursor relationships in the ambient atmosphere, *Journal of Geophysical Research*, 97, 6037, <https://doi.org/10.1029/91JD03014>, <http://doi.wiley.com/10.1029/91JD03014>, 1992.
- Charlsson, R. J., Lovelock, J., Andreae, M. O., and Warren, S. G.: Oceanic phytoplankton, atmospheric sulphur, cloud albedo and climate, *Nature*, 326, 1987.
- 30 Chen, H. and Finlayson-Pitts, B. J.: New Particle Formation from Methanesulfonic Acid and Amines/Ammonia as a Function of Temperature, *Environmental Science and Technology*, 51, 243–252, <https://doi.org/10.1021/acs.est.6b04173>, 2017.
- Chin, M., Jacob, D. J., Gardner, G. M., Foreman-Fowler, M. S., Spiro, P. A., and Savoie, D. L.: A global three-dimensional model of tropospheric sulfate, *Journal of Geophysical Research: Atmospheres*, 101, 18 667–18 690, <https://doi.org/10.1029/96JD01221>, 1996.
- Collins, J. W., Lamarque, J. F., Schulz, M., Boucher, O., Eyring, V., Hegglin, I. M., Maycock, A., Myhre, G., Prather, M., Shindell, D., and Smith, J. S.: AerChemMIP: Quantifying the effects of chemistry and aerosols in CMIP6, *Geoscientific Model Development*, 10, 585–607, <https://doi.org/10.5194/gmd-10-585-2017>, 2017.
- 35

- Collins, W. J., Derwent, R. G., Johnson, C. E., and Stevenson, D. S.: The oxidation of organic compounds in the troposphere and their global warming potentials, *Climatic Change*, 52, 453–479, <https://doi.org/10.1023/A:1014221225434>, 2002.
- Crutzen, P. and Lelieveld, J.: HUMAN IMPACTS ON ATMOSPHERIC CHEMISTRY, *Annual Review of Earth and Planetary Sciences*, 29, 17–45, 2001.
- 5 Dentener, F., Kinne, S., Bond, T., Boucher, O., Cofala, J., Generoso, S., Ginoux, P., Gong, S., Hoelzemann, J. J., Ito, A., Marelli, L., Penner, J. E., Putaud, J. P., Textor, C., Schulz, M., Van Der Werf, G. R., and Wilson, J.: Emissions of primary aerosol and precursor gases in the years 2000 and 1750 prescribed data-sets for AeroCom, *Atmospheric Chemistry and Physics*, 6, 4321–4344, <https://doi.org/10.5194/acp-6-4321-2006>, 2006.
- Emmons, L. K., Walters, S., Hess, P. G., Lamarque, J.-F., Pfister, G. G., Fillmore, D., Granier, C., Guenther, A., Kinnison, D., Laeple, T., Orlando, J., Tie, X., Tyndall, G., Wiedinmyer, C., Baughcum, S. L., and Kloster, S.: Description and evaluation of the Model for Ozone and Related chemical Tracers, version 4 (MOZART-4), *Geoscientific Model Development Discussions*, 3, 43–67, <https://doi.org/10.5194/gmdd-2-1157-2009>, 2010.
- 10 Gettelman, A.: Putting the clouds back in aerosol-cloud interactions, *Atmospheric Chemistry and Physics*, 15, 12397–12411, <https://doi.org/10.5194/acp-15-12397-2015>, 2015.
- 15 Gettelman, A. and Morrison, H.: Advanced two-moment bulk microphysics for global models. Part I: Off-line tests and comparison with other schemes, *Journal of Climate*, 28, 1268–1287, <https://doi.org/10.1175/JCLI-D-14-00102.1>, 2015.
- Gettelman, A., Morrison, H., Santos, S., Bogenschutz, P., and Caldwell, P. M.: Advanced two-moment bulk microphysics for global models. Part II: Global model solutions and aerosol-cloud interactions, *Journal of Climate*, 28, 1288–1307, <https://doi.org/10.1175/JCLI-D-14-00103.1>, 2015.
- 20 Ghan, S. J.: Technical note: Estimating aerosol effects on cloud radiative forcing, *Atmospheric Chemistry and Physics*, 13, 9971–9974, <https://doi.org/10.5194/acp-13-9971-2013>, 2013.
- Gordon, H., Sengupta, K., Rap, A., Duplissy, J., Frege, C., Williamson, C., Heinritzi, M., Simon, M., Yan, C., Almeida, J., Tröstl, J., Nieminen, T., Ortega, I. K., Wagner, R., Dunne, E. M., Adamov, A., Amorim, A., Bernhammer, A.-K., Bianchi, F., Breitenlechner, M., Brilke, S., Chen, X., Craven, J. S., Dias, A., Ehrhart, S., Fischer, L., Flagan, R. C., Franchin, A., Fuchs, C., Guida, R., Hakala, J., Hoyle, C. R., Jokinen, T., Junninen, H., Kangasluoma, J., Kim, J., Kirkby, J., Krapf, M., Kürten, A., Laaksonen, A., Lehtipalo, K., Makhmutov, V., Mathot, S., Molteni, U., Monks, S. A., Onnela, A., Peräkylä, O., Piel, F., Petäjä, T., Praplan, A. P., Pringle, K. J., Richards, N. A. D., Rissanen, M. P., Rondo, L., Sarnela, N., Schobesberger, S., Scott, C. E., Seinfeld, J. H., Sharma, S., Sipilä, M., Steiner, G., Stozhkov, Y., Stratmann, F., Tomé, A., Virtanen, A., Vogel, A. L., Wagner, A. C., Wagner, P. E., Weingartner, E., Wimmer, D., Winkler, P. M., Ye, P., Zhang, X., Hansel, A., Dommen, J., Donahue, N. M., Worsnop, D. R., Baltensperger, U., Kulmala, M., Curtius, J., and Carslaw, K. S.:
- 30 Reduced anthropogenic aerosol radiative forcing caused by biogenic new particle formation, *Proceedings of the National Academy of Sciences*, 113, <https://doi.org/10.1073/pnas.1602360113>, 2016.
- Guenther, A. B., Jiang, X., Heald, C. L., Sakulyanontvittaya, T., Duhl, T., Emmons, L. K., and Wang, X.: The model of emissions of gases and aerosols from nature version 2.1 (MEGAN2.1): An extended and updated framework for modeling biogenic emissions, *Geoscientific Model Development*, 5, 1471–1492, <https://doi.org/10.5194/gmd-5-1471-2012>, 2012.
- 35 Hoose, C., Lohmann, U., Erdin, R., and Tegen, I.: The global influence of dust mineralogical composition on heterogeneous ice nucleation in mixed-phase clouds, *Environmental Research Letters*, 3, <https://doi.org/10.1088/1748-9326/3/2/025003>, 2008.
- Hoose, C., Kristjánsson, J. E., Iversen, T., Kirkevåg, A., Seland, and Gettelman, A.: Constraining cloud droplet number concentration in GCMs suppresses the aerosol indirect effect, *Geophysical Research Letters*, 36, 1–5, <https://doi.org/10.1029/2009GL038568>, 2009.

- Hoose, C., Kristjánsson, J. E., Chen, J.-P., and Hazra, A.: A Classical-Theory-Based Parameterization of Heterogeneous Ice Nucleation by Mineral Dust, Soot, and Biological Particles in a Global Climate Model, *Journal of the Atmospheric Sciences*, 67, 2483–2503, <https://doi.org/10.1175/2010JAS3425.1>, 2010.
- Iversen, T., Bentsen, M., Bethke, I., Debernard, J. B., Kirkevåg, A., Seland, Ø., Drange, H., Kristjánsson, J. E., Medhaug, I., Sand, M., and Seierstad, I. A.: The Norwegian Earth System Model, NorESM1-M – Part 2: Climate response and scenario projections, *Geoscientific Model Development Discussions*, 5, 2933–2998, <https://doi.org/10.5194/gmdd-5-2933-2012>, <http://www.geosci-model-dev-discuss.net/5/2933/2012/>, 2013.
- Jaenicke, R.: Natural Aerosols, *Annals of the New York Academy of Sciences*, 338, 317–329, <https://doi.org/10.1111/j.1749-6632.1980.tb17129.x>, 1980.
- 10 Jokinen, T., Berndt, T., Makkonen, R., Kerminen, V.-M., Junninen, H., Paasonen, P., Stratmann, F., Herrmann, H., Guenther, A. B., Worsnop, D. R., Kulmala, M., Ehn, M., and Sipilä, M.: Production of extremely low volatile organic compounds from biogenic emissions: Measured yields and atmospheric implications, *Proceedings of the National Academy of Sciences*, 112, 7123–7128, <https://doi.org/10.1073/pnas.1423977112>, <http://www.pnas.org/lookup/doi/10.1073/pnas.1423977112>, 2015.
- Khan, M. A. H., Cooke, M. C., Utembe, S. R., Archibald, A. T., Derwent, R. G., Xiao, P., Percival, C. J., Jenkin, M. E., Morris, W. C., and Shallcross, D. E.: Global modeling of the nitrate radical (NO₃) for present and pre-industrial scenarios, *Atmospheric Research*, 164–165, 347–357, <https://doi.org/10.1016/j.atmosres.2015.06.006>, 2015.
- Kirkevåg, A., Iversen, T., Seland, Ø., Debernard, J. B., Storelvmo, T., and Kristjánsson, J. E.: Aerosol-cloud-climate interactions in the climate model CAM-Oslo, *Tellus, Series A: Dynamic Meteorology and Oceanography*, 60 A, 492–512, <https://doi.org/10.1111/j.1600-0870.2008.00313.x>, 2008.
- 20 Kirkevåg, A., Iversen, T., Seland, Ø., Hoose, C., Kristjánsson, J. E., Struthers, H., Ekman, A. M. L., Ghan, S., Griesfeller, J., Nilsson, E. D., and Schulz, M.: Aerosol-climate interactions in the Norwegian Earth System Model - NorESM1-M, *Geoscientific Model Development*, 6, 207–244, <https://doi.org/https://doi.org/10.5194/gmd-6-207-2013>, 2013.
- Kirkevåg, A., Grini, A., Olivie, D., Seland, Ø., Alterskjær, K., Hummel, M., Karset, I. H. H., Lewinhal, A., Xiaohong, L., Makkonen, R., Bethke, I., Griesfeller, J., Schulz, M., and Iversen, T.: A production-tagged aerosol module for earth system models - extensions and updates for CAM5.3-Oslo. Manuscript in preparation, 2018.
- 25 Kooperman, G. J., Pritchard, M. S., Ghan, S. J., Wang, M., Somerville, R. C. J., and Russell, L. M.: Constraining the influence of natural variability to improve estimates of global aerosol indirect effects in a nudged version of the Community Atmosphere Model 5, *Journal of Geophysical Research Atmospheres*, 117, <https://doi.org/10.1029/2012JD018588>, 2012.
- Kroll, J. H., Ng, N. L., Murphy, S. M., Flagan, R. C., and Seinfeld, J. H.: Secondary organic aerosol formation from isoprene photooxidation under high-NO_x conditions, *Geophysical Research Letters*, 32, <https://doi.org/10.1029/2005GL023637>, <http://doi.wiley.com/10.1029/2005GL023637>, 2005.
- 30 Lamarque, J. F., Bond, T. C., Eyring, V., Granier, C., Heil, A., Klimont, Z., Lee, D., Liou, S., Mieville, A., Owen, B., Schultz, M. G., Shindell, D., Smith, S. J., Stehfest, E., Van Aardenne, J., Cooper, O. R., Kainuma, M., Mahowald, N., McConnell, J. R., Naik, V., Riahi, K., and Van Vuuren, D. P.: Historical (1850–2000) gridded anthropogenic and biomass burning emissions of reactive gases and aerosols: Methodology and application, *Atmospheric Chemistry and Physics*, 10, 7017–7039, <https://doi.org/10.5194/acp-10-7017-2010>, 2010.
- 35 Lamarque, J. F., Emmons, L. K., Hess, P. G., Kinnison, D. E., Tilmes, S., Vitt, F., Heald, C. L., Holland, E. A., Lauritzen, P. H., Neu, J., Orlando, J. J., Rasch, P. J., and Tyndall, G. K.: CAM-chem: Description and evaluation of interactive atmospheric chemistry in the Community Earth System Model, *Geoscientific Model Development*, 5, 369–411, <https://doi.org/10.5194/gmd-5-369-2012>, 2012.

- Lee, A., Goldstein, A. H., Kroll, J. H., Ng, N. L., Varutbangkul, V., Flagan, R. C., and Seinfeld, J. H.: Gas-phase products and secondary aerosol yields from the photooxidation of 16 different terpenes, *Journal of Geophysical Research Atmospheres*, 111, 1–25, <https://doi.org/10.1029/2006JD007050>, 2006.
- Lehtinen, K. E., Dal Maso, M., Kulmala, M., and Kerminen, V. M.: Estimating nucleation rates from apparent particle formation rates and vice versa: Revised formulation of the Kerminen-Kulmala equation, *Journal of Aerosol Science*, 38, 988–994, <https://doi.org/10.1016/j.jaerosci.2007.06.009>, 2007.
- Liu, X., Easter, R. C., Ghan, S. J., Zaveri, R., Rasch, P., Shi, X., Lamarque, J. F., Gettelman, A., Morrison, H., Vitt, F., Conley, A., Park, S., Neale, R., Hannay, C., Ekman, A. M., Hess, P., Mahowald, N., Collins, W., Iacono, M. J., Bretherton, C. S., Flanner, M. G., and Mitchell, D.: Toward a minimal representation of aerosols in climate models: Description and evaluation in the Community Atmosphere Model CAM5, *Geoscientific Model Development*, 5, 709–739, <https://doi.org/10.5194/gmd-5-709-2012>, 2012.
- Liu, X., Ma, P. L., Wang, H., Tilmes, S., Singh, B., Easter, R. C., Ghan, S. J., and Rasch, P. J.: Description and evaluation of a new four-mode version of the Modal Aerosol Module (MAM4) within version 5.3 of the Community Atmosphere Model, *Geoscientific Model Development*, 9, 505–522, <https://doi.org/10.5194/gmd-9-505-2016>, 2016.
- Lohmann, U.: Global anthropogenic aerosol effects on convective clouds in ECHAM5-HAM, *Atmospheric Chemistry and Physics*, 8, 2115–2131, <https://doi.org/10.5194/acpd-7-14639-2007>, 2008.
- Lohmann, U.: Anthropogenic Aerosol Influences on Mixed-Phase Clouds, *Current Climate Change Report*, 3, 32–44, <https://doi.org/10.1007/s40641-017-0059-9>, 2017.
- Lohmann, U. and Diehl, K.: Sensitivity Studies of the Importance of Dust Ice Nuclei for the Indirect Aerosol Effect on Stratiform Mixed-Phase Clouds, *Journal of the Atmospheric Sciences*, 63, 968–982, <https://doi.org/10.1175/JAS3662.1>, 2006.
- Lohmann, U. and Ferrachat, S.: Impact of parametric uncertainties on the present-day climate and on the anthropogenic aerosol effect, *Atmospheric Chemistry and Physics*, 10, 11 373–11 383, <https://doi.org/10.5194/acp-10-11373-2010>, 2010.
- Lohmann, U., Feichter, J., Penner, J., and Leaitch, R.: Indirect effect of sulfate and carbonaceous aerosols: A mechanistic treatment, *Journal of Geophysical Research: Atmospheres*, 105, 12 193–12 206, <https://doi.org/10.1029/1999JD901199>, <http://doi.wiley.com/10.1029/1999JD901199>, 2000.
- Makkonen, R., Seland, Ø., Kirkevåg, A., Iversen, T., and Kristjánsson, J. E.: Evaluation of aerosol number concentrations in NorESM with improved nucleation parameterization, *Atmospheric Chemistry and Physics*, 14, 5127–5152, <https://doi.org/10.5194/acp-14-5127-2014>, 2014.
- Menon, S. and Rotstayn, L.: The radiative influence of aerosol effects on liquid-phase cumulus and stratiform clouds based on sensitivity studies with two climate models, *Climate Dynamics*, 27, 345–356, <https://doi.org/10.1007/s00382-006-0139-3>, 2006.
- Morrison, H. and Gettelman, A.: A new two-moment bulk stratiform cloud microphysics scheme in the community atmosphere model, version 3 (CAM3). Part I: Description and numerical tests, *Journal of Climate*, 21, 3642–3659, <https://doi.org/10.1175/2008JCLI2105.1>, 2008.
- Murray, L. T., Mickley, L. J., Kaplan, J. O., Sofen, E. D., Pfeiffer, M., and Alexander, B.: Factors controlling variability in the oxidative capacity of the troposphere since the Last Glacial Maximum, *Atmospheric Chemistry and Physics*, 14, 3589–3622, <https://doi.org/10.5194/acp-14-3589-2014>, 2014.
- Myhre, G., Shindell, D., Bréon, F.-M., Collins, W., Fuglestedt, J., Huang, J., Koch, D., Lamarque, J.-F., Lee, D., Mendoza, B., Nakajima, T., Robock, A., Stephens, G., Takemura, T., and Zhang, H.: Anthropogenic and Natural Radiative Forcing, in: *Climate Change 2013: The Physical Science Basis. Contribution of Working Group I to the Fifth Assessment Report of the Intergovernmental Panel on Climate*

- Change, edited by Stocker, T., D. Qin, G.-K., Plattner, M., Tignor, S., Allen, J., Boschung, A., Nauels, Y., Xia, V., Midgley, B., and P.M., chap. 7, pp. 659–740, Cambridge University Press, Cambridge, United Kingdom and New York, NY, USA, <https://doi.org/10.1017/CBO9781107415324.018>, 2013.
- Naik, V., Horowitz, L. W., Fiore, A. M., Ginoux, P., Mao, J., and Aghedo, A. M.: Impact of preindustrial to present-day changes in short-lived pollutant emissions on atmospheric composition and climate forcing, *Journal of Geophysical Research Atmospheres*, 118, 8086–8110, <https://doi.org/10.1002/jgrd.50608>, 2013a.
- Naik, V., Voulgarakis, A., Fiore, A. M., Horowitz, L. W., Lamarque, J. F., Lin, M., Prather, M. J., Young, P. J., Bergmann, D., Cameron-Smith, P. J., Cionni, I., Collins, W. J., Dalsøren, S. B., Doherty, R., Eyring, V., Faluvegi, G., Folberth, G. A., Josse, B., Lee, Y. H., MacKenzie, I. A., Nagashima, T., Van Noije, T. P., Plummer, D. A., Righi, M., Rumbold, S. T., Skeie, R., Shindell, D. T., Stevenson, D. S., Strode, S., Sudo, K., Szopa, S., and Zeng, G.: Preindustrial to present-day changes in tropospheric hydroxyl radical and methane lifetime from the Atmospheric Chemistry and Climate Model Intercomparison Project (ACCMIP), *Atmospheric Chemistry and Physics*, 13, 5277–5298, <https://doi.org/10.5194/acp-13-5277-2013>, 2013b.
- Neale, R. B., Chen, C.-C., Gettelman, A., Lauritzen, P. H., Park, S., Williamson, D. L., Conley, A. J., Garcia, R., Kinnison, D., Lamarque, J.-F., Marsh, D., Mills, M., Smith, A. K., Tilmes, S., Vitt, F., Morrison, H., Cameron-Smith, P., Collins, W. D., Iacono, M. J., Easter, R. C., Ghan, S. J., Liu, X., Rasch, P. J., and Taylor, M. A.: Description of the NCAR Community Atmosphere Model (CAM 5.0), 2012.
- Neubauer, D., Lohmann, U., Hoose, C., and Frontoso, M. G.: Impact of the representation of marine stratocumulus clouds on the anthropogenic aerosol effect, *Atmospheric Chemistry and Physics*, 14, 11 997–12 022, <https://doi.org/10.5194/acp-14-11997-2014>, 2014.
- Nightingale, P. D., Malin, G., Law, C. S., Watson, A. J., Liss, P. S., Liddicoat, M. I., Boutin, J., and Upstill-Goddard, R. C.: In situ evaluation of air-sea gas exchange parameterizations using novel conservative and volatile tracers, *Global Biogeochemical Cycles*, 14, 373–387, <https://doi.org/10.1029/1999GB900091>, 2000.
- Oleson, K. W., Lawrence, D. M., Authors, L., Bonan, G. B., Drewniak, B., Huang, M., Koven, C. D., Levis, S., Li, F., Riley, W. J., Subin, Z. M., Swenson, S. C., Thornton, P. E., Bozbiyik, A., Fisher, R., Heald, C. L., Kluzek, E., Lamarque, J.-F., Lawrence, P. J., Leung, L. R., Lipscomb, W., Muszala, S., Ricciuto, D. M., Sacks, W., Sun, Y., Tang, J., and Yang, Z.-L.: Technical Description of version 4.5 of the Community Land Model (CLM), <http://library.ucar.edu/research/publish-technote>, 2013.
- Paasonen, P., Nieminen, T., Asmi, E., Manninen, H. E., Petäjä, T., Plass-Dülmer, C., Flentje, H., Birmili, W., Wiedensohler, A., Hörrak, U., Metzger, A., Hamed, A., Laaksonen, A., Facchini, M. C., Kerminen, V. M., and Kulmala, M.: On the roles of sulphuric acid and low-volatility organic vapours in the initial steps of atmospheric new particle formation, *Atmospheric Chemistry and Physics*, 10, 11 223–11 242, <https://doi.org/10.5194/acp-10-11223-2010>, 2010.
- Parrish, D. D., Lamarque, J. F., Naik, V., Horowitz, L., Shindell, D. T., Staehelin, J., Derwent, R., Cooper, O. R., Tanimoto, H., Volz-Thomas, A., Gilge, S., Scheel, H. E., Steinbacher, M., and Fröhlich, M.: Long-term changes in lower tropospheric baseline ozone concentrations: Comparing chemistry-climate models and observations at northern midlatitudes, *Journal of Geophysical Research*, 119, 5719–5736, <https://doi.org/10.1002/2013JD021435>, 2014.
- Pavelin, E. G., Johnson, C. E., Rughooputh, S., and Toumi, R.: Evaluation of pre-industrial surface ozone measurements made using Schönbain’s method, *Atmospheric Environment*, 33, 919–929, [https://doi.org/10.1016/S1352-2310\(98\)00257-X](https://doi.org/10.1016/S1352-2310(98)00257-X), 1999.
- Pincus, R. and Baker, M. B.: Effect of precipitation on the albedo susceptibility of clouds in the marine boundary layer, *Nature*, 372, 250–252, 1994.
- Prinn, R. G.: THE CLEANSING CAPACITY OF THE ATMOSPHERE, *Annual Review of Environment and Resources*, 28, 29–57, <https://doi.org/10.1146/annurev.energy.28.011503.163425>, 2003.

- Salzmann, M., Ming, Y., Golaz, J. C., Ginoux, P. A., Morrison, H., Gettelman, A., Kramer, M., and Donner, L. J.: Two-moment bulk stratiform cloud microphysics in the GFDL AM3 GCM: Description, evaluation, and sensitivity tests, *Atmospheric Chemistry and Physics*, 10, 8037–8064, <https://doi.org/10.5194/acp-10-8037-2010>, 2010.
- Sant, V., Posselt, R., and Lohmann, U.: Prognostic precipitation with three liquid water classes in the ECHAM5-HAM GCM, *Atmospheric Chemistry and Physics*, 15, 8717–8738, <https://doi.org/10.5194/acp-15-8717-2015>, 2015.
- Seinfeld, J. H.: Urban Air Pollution: State of the Science, *Science*, 243, 745–752, <https://doi.org/10.1126/science.243.4892.745>, <http://www.sciencemag.org/cgi/doi/10.1126/science.243.4892.745>, 1989.
- Seinfeld, J. H. and Pandis, S. N.: *Atmospheric Chemistry and Physics: From Air Pollution to Climate Change*, Wiley, third edit edn., 2016.
- Shaw, S. L., Gantt, B., and Meskhidze, N.: Production and Emissions of Marine Isoprene and Monoterpenes: A Review, *Advances in Meteorology*, 2010, 1–24, <https://doi.org/10.1155/2010/408696>, <http://www.hindawi.com/journals/amete/2010/408696/>, 2010.
- Spivakovsky, C. M., Logan, J. A., Montzka, S. A., Balkanski, Y. J., Foreman-Fowler, M., Jones, D. B. A., Horowitz, L. W., Fusco, A. C., Brenninkmeijer, C. A. M., Prather, M. J., Wofsy, S. C., and McElroy, M. B.: Three-dimensional climatological distribution of tropospheric OH: Update and evaluation, *Journal of Geophysical Research: Atmospheres*, 105, 8931–8980, <https://doi.org/10.1029/1999JD901006>, <http://doi.wiley.com/10.1029/1999JD901006>, 2000.
- 15 Spracklen, D. V., Jimenez, J. L., Carslaw, K. S., Worsnop, D. R., Evans, M. J., Mann, G. W., Zhang, Q., Canagaratna, M. R., Allan, J., Coe, H., McFiggans, G., Rap, A., and Forster, P.: Aerosol mass spectrometer constraint on the global secondary organic aerosol budget, *Atmospheric Chemistry and Physics*, 11, 12 109–12 136, <https://doi.org/10.5194/acp-11-12109-2011>, 2011.
- Storelvmo, T.: Aerosol Effects on Climate via Mixed-Phase and Ice Clouds, *Annual Review of Earth and Planetary Sciences*, 45, 199–222, <https://doi.org/10.1146/annurev-earth-060115-012240>, <http://www.annualreviews.org/doi/10.1146/annurev-earth-060115-012240>, 2017.
- 20 Storelvmo, T., Kristjánsson, J. E., Lohmann, U., Iversen, T., Kirkevåg, A., and Seland: Modeling of the Wegener-Bergeron-Findeisen process - Implications for aerosol indirect effects, *Environmental Research Letters*, 3, <https://doi.org/10.1088/1748-9326/3/4/045001>, 2008.
- Tie, X., Brasseur, G., Emmons, L., Horowitz, L., and Kinnison, D.: Effects of aerosols on tropospheric oxidants: A global model study, *Journal of Geophysical Research: Atmospheres*, 106, 22 931–22 964, <https://doi.org/10.1029/2001JD900206>, <http://doi.wiley.com/10.1029/2001JD900206>, 2001.
- 25 Tonttila, J., Jarvinen, H., and Raisanen, P.: Explicit representation of subgrid variability in cloud microphysics yields weaker aerosol indirect effect in the ECHAM5-HAM2 climate model, *Atmospheric Chemistry and Physics*, 15, 703–714, <https://doi.org/10.5194/acp-15-703-2015>, 2015.
- Tsigradis, K., Krol, M., Dentener, F. J., Balkanski, Y., Lathière, J., Metzger, S., Hauglustaine, D. A., and Kanakidou, M.: Change in global aerosol composition since preindustrial times, *Atmospheric Chemistry and Physics*, 6, 5143–5162, [https://doi.org/10.5194/acp-6-5143-](https://doi.org/10.5194/acp-6-5143-2006)
- 30 2006, 2006.
- Tsigradis, K., Daskalakis, N., Kanakidou, M., Adams, P. J., Artaxo, P., Bahadur, R., Balkanski, Y., Bauer, S. E., Bellouin, N., Benedetti, A., Bergman, T., Bernsten, T. K., Beukes, J. P., Bian, H., Carslaw, K. S., Chin, M., Curci, G., Diehl, T., Easter, R. C., Ghan, S. J., Gong, S. L., Hodzic, A., Hoyle, C. R., Iversen, T., Jathar, S., Jimenez, J. L., Kaiser, J. W., Kirkevåg, A., Koch, D., Kokkola, H., H Lee, Y., Lin, G., Liu, X., Luo, G., Ma, X., Mann, G. W., Mihalopoulos, N., Morcrette, J. J., Müller, J. F., Myhre, G., Myriokefalitakis, S., Ng, N. L., O'donnell, D., Penner, J. E., Pozzoli, L., Pringle, K. J., Russell, L. M., Schulz, M., Sciare, J., Seland, Shindell, D. T., Sillman, S., Skeie, R. B., Spracklen, D., Stavrou, T., Steenrod, S. D., Takemura, T., Tiitta, P., Tilmes, S., Tost, H., Van Noije, T., Van Zyl, P. G., Von Salzen, K., Yu, F., Wang, Z., Wang, Z., Zaveri, R. A., Zhang, H., Zhang, K., Zhang, Q., and Zhang, X.: The AeroCom evaluation and intercomparison

- of organic aerosol in global models, *Atmospheric Chemistry and Physics*, 14, 10 845–10 895, <https://doi.org/10.5194/acp-14-10845-2014>, 2014.
- Twomey, S.: The Influence of Pollution on the Shortwave Albedo of Clouds, *Journal of the Atmospheric Sciences*, 34, 1149–1152, [https://doi.org/https://doi.org/10.1175/1520-0469\(1977\)034<1149:TIOPO>2.0.CO;2](https://doi.org/https://doi.org/10.1175/1520-0469(1977)034<1149:TIOPO>2.0.CO;2), 1977.
- 5 Twomey, S.: Aerosols, clouds and radiation, *Atmospheric Environment Part A, General Topics*, 25, 2435–2442, [https://doi.org/10.1016/0960-1686\(91\)90159-5](https://doi.org/10.1016/0960-1686(91)90159-5), 1991.
- Unger, N.: Human land-use-driven reduction of forest volatiles cools global climate, *Nature Climate Change*, 4, 907–910, <https://doi.org/10.1038/nclimate2347>, 2014.
- Vehkamäki, H., Kulmala, M., Napari, I., Lehtinen, K. E. J., Timmreck, C., Noppel, M., and Laaksonen, A.: An improved parameterization for sulfuric acid–water nucleation rates for tropospheric and stratospheric conditions, *Journal of Geophysical Research*, 107, 4622, <https://doi.org/10.1029/2002JD002184>, <http://doi.wiley.com/10.1029/2002JD002184>, 2002.
- 10 Volz, A. and Kley, D.: Evaluation of the Montsouris series of ozone measurements made in the nineteenth century, <https://doi.org/10.1038/332240a0>, <http://www.nature.com/doi/finder/10.1038/332240a0>, 1988.
- Wang, M., Ghan, S., Ovchinnikov, M., Liu, X., Easter, R., Kassianov, E., Qian, Y., and Morrison, H.: Aerosol indirect effects in a multi-scale aerosol-climate model PNNL-MMF, *Atmospheric Chemistry and Physics*, 11, 5431–5455, <https://doi.org/10.5194/acp-11-5431-2011>, 2011.
- 15 Wang, Y. and Jacob, D. J.: Anthropogenic forcing on tropospheric ozone and OH since preindustrial times, *JOURNAL OF GEOPHYSICAL RESEARCH*, 103, 31,123–31,135, <https://doi.org/10.1029/1998JD100004>, 1998.
- Wang, Y., Liu, X., Hoese, C., and Wang, B.: Different contact angle distributions for heterogeneous ice nucleation in the Community Atmospheric Model version 5, *Atmospheric Chemistry and Physics*, 14, 10 411–10 430, <https://doi.org/10.5194/acp-14-10411-2014>, 2014.
- 20 Wayne, R. P., Barnes, I., Biggs, P., Burrows, J. P., Canosa-Mas, C. E., Hjorth, J., Le Bras, G., Moortgat, G. K., Perner, D., Poulet, G., Restelli, G., and Sidebottom, H.: The nitrate radical: Physics, chemistry, and the atmosphere, *Atmospheric Environment. Part A. General Topics*, 25, 1–203, [https://doi.org/10.1016/0960-1686\(91\)90192-A](https://doi.org/10.1016/0960-1686(91)90192-A), 1991.
- Williams, J., de Reus, M., Krejci, R., Fischer, H., and Ström, J.: Application of the variability-size relationship to atmospheric aerosol studies: estimating aerosol lifetimes and ages, *Atmospheric Chemistry and Physics Discussions*, 2, 43–74, <https://doi.org/10.5194/acpd-2-43-2002>, 2002.
- 25 Willis, M. D., Burkart, J., Thomas, J. L., Köllner, F., Schneider, J., Bozem, H., Hoor, P. M., Aliabadi, A. A., Schulz, H., Herber, A. B., Leaitch, W. R., and Abbatt, J. P.: Growth of nucleation mode particles in the summertime Arctic: A case study, *Atmospheric Chemistry and Physics*, 16, 7663–7679, <https://doi.org/10.5194/acp-16-7663-2016>, 2016.
- 30 Woodhouse, M. T., Carslaw, K. S., Mann, G. W., Vallina, S. M., Vogt, M., Halloran, P. R., and Boucher, O.: Low sensitivity of cloud condensation nuclei to changes in the sea-air flux of dimethyl-sulphide, *Atmospheric Chemistry and Physics*, 10, 7545–7559, <https://doi.org/10.5194/acp-10-7545-2010>, 2010.
- Young, P. J., Archibald, A. T., Bowman, K. W., Lamarque, J.-F., Naik, V., Stevenson, D. S., Tilmes, S., Voulgarakis, A., Wild, O., Bergmann, D., Cameron-Smith, P., Cionni, I., Collins, W. J., Dalsøren, S. B., Doherty, R. M., Eyring, V., Faluvegi, G., Horowitz, L. W., Josse, B., Lee, Y. H., MacKenzie, I. A., Nagashima, T., Plummer, D. A., Righi, M., Rumbold, S. T., Skeie, R. B., Shindell, D. T., Strode, S. A., Sudo, K., Szopa, S., and Zeng, G.: Pre-industrial to end 21st century projections of tropospheric ozone from the Atmospheric Chemistry and Climate Model Intercomparison Project (ACCMIP), *Atmospheric Chemistry and Physics*, 13, 2063–2090, <https://doi.org/10.5194/acp-13-2063-2013>, 2013.

Yun, Y. and Penner, J. E.: An evaluation of the potential radiative forcing and climatic impact of marine organic aerosols as heterogeneous ice nuclei, *Geophysical Research Letters*, 40, 4121–4126, <https://doi.org/10.1002/grl.50794>, 2013.

Zhang, K., Wan, H., Liu, X., Ghan, S. J., Kooperman, G. J., Ma, P. L., Rasch, P. J., Neubauer, D., and Lohmann, U.: Technical note: On the use of nudging for aerosol-climate model intercomparison studies, *Atmospheric Chemistry and Physics*, 14, 8631–8645,

5 <https://doi.org/10.5194/acp-14-8631-2014>, 2014.

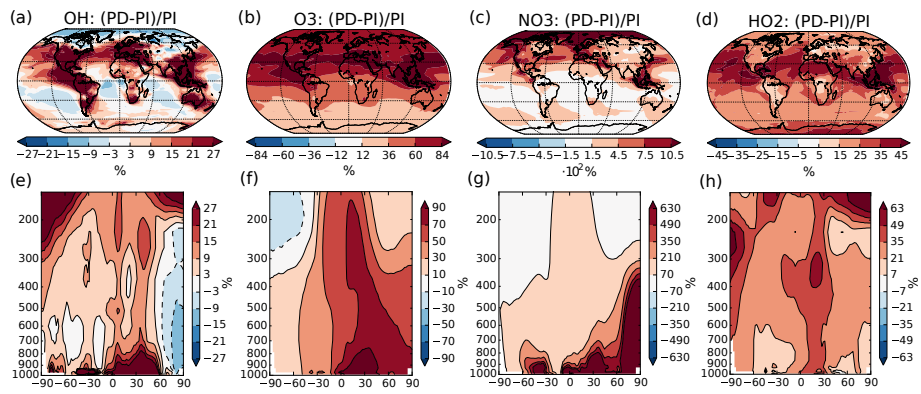


Figure 1. Percent-wise change in the annual mean oxidant mixing ratio (mol/mol) between PI and PD in the dataset from Lamarque et al. (2010) used in this study. Top: mean change from surface and up to 550 hPa. Bottom: zonal mean change. Please note the different scales on the color bars.

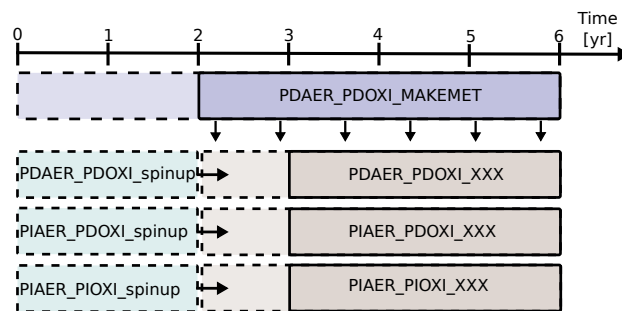


Figure 2. Overview of how the simulations were carried out. PDAER_PDOXI_MAKEMET produced meteorology for the other simulations from its last four years. Dashed lines show the part of the simulations used as [spin-up](#). Horizontal arrows show that the [cases simulations](#) to the right of the arrow restarted from the already spun up [ease-simulation](#) to the left. The [spin-up](#) cases were not nudged, but started with free running meteorology from the same state as PDAER_PDOXI_MAKEMET. XXX refers to either ORG (original model setup), or the name of the sensitivity tests described in Sect. 3.2 and 4.3.

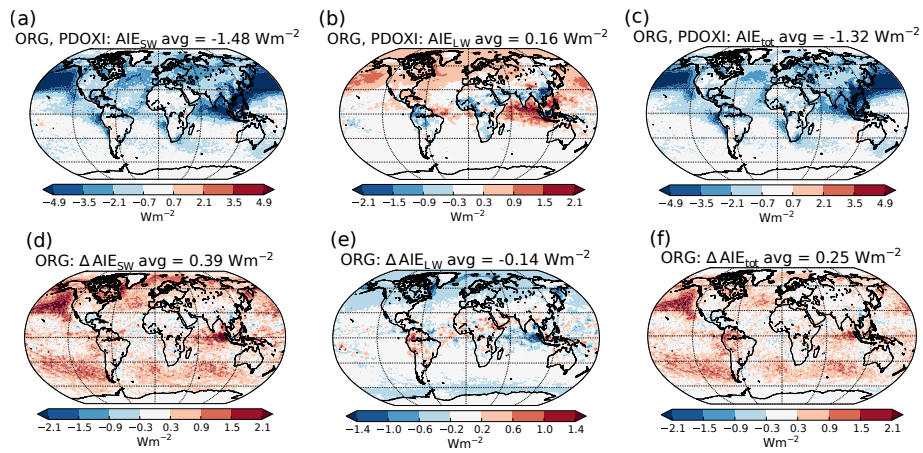


Figure 3. Top: PD-PI aerosol indirect effect when using the standard setup with PD-oxidants in both simulations. Left: shortwave, middle: longwave, right: total. Bottom: ~~Differences~~ differences in the PD-PI indirect ~~effects~~ effect between simulations performed with PI- and PD-oxidants in the PI-simulation.

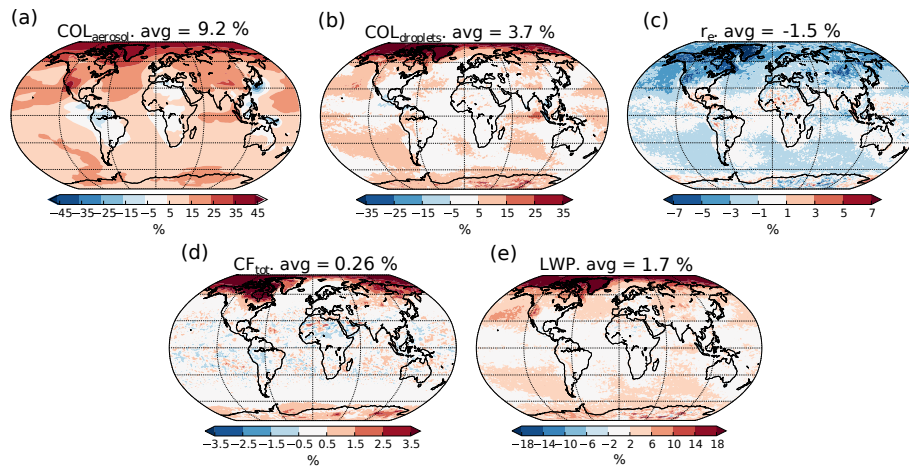


Figure 4. Relative change in aerosol and cloud properties in the PI-simulation when switching from PD- to PI-oxidants. (a) Column number of aerosols, (b) column number of cloud droplets, (c) effective radius of cloud droplets in the cloud top layer, (d) total cloud fraction, and (e) total gridbox averaged liquid water path.

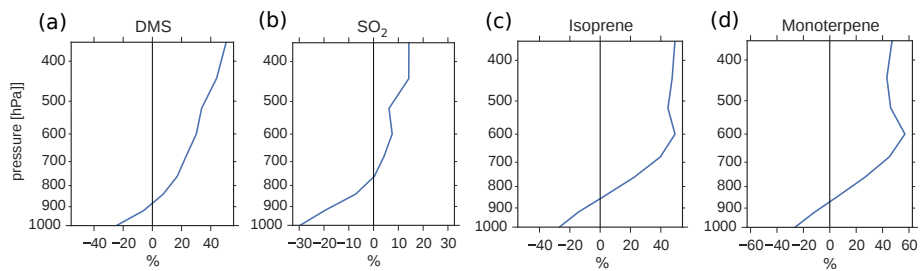


Figure 5. Global mean relative change in chemical loss of (a) DMS, (b) SO_2 , (c) isoprene and (d) monoterpene when switching from PD- to PI-oxidants in the PI-simulation.

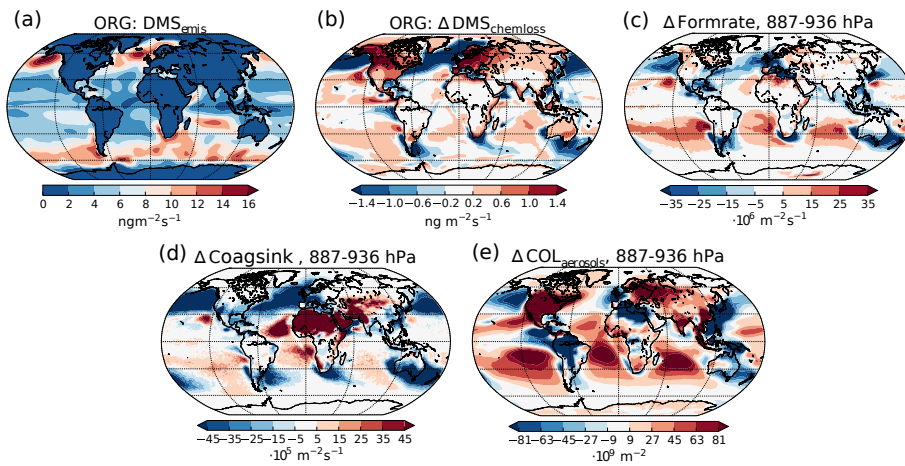


Figure 6. (a) Emission rate of DMS (same for both PI-simulations). (b) Difference in net chemical loss of DMS through oxidation (c) Difference in aerosol formation rate in the layer 887-936 hPa. (d) Difference in the coagulation sink during nucleation in the layer 887-936 hPa. (e) Difference in column burden of aerosols in the layer 887-936 hPa. All differences show values from the PI-simulation using PI-oxidants minus values from the PI-simulation using PD-oxidants.

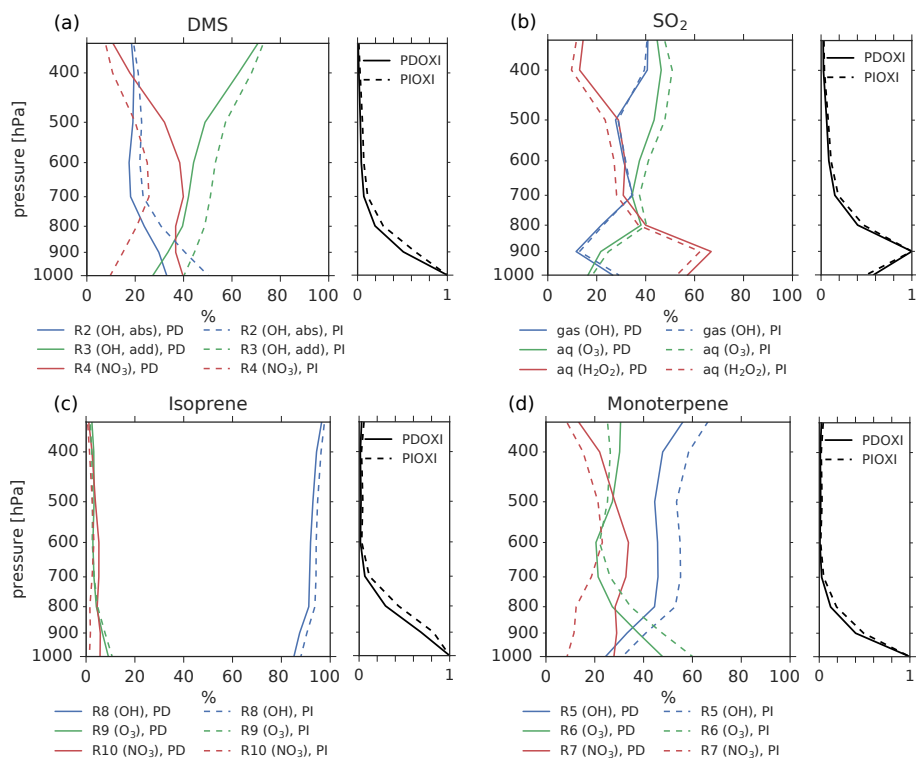


Figure 7. The left panel of each figure shows the importance of different oxidant reactions at different levels for (a) DMS, (b) SO₂, (c) isoprene and (d) monoterpene. Solid lines: PD-oxidants, dashed lines: PI-oxidants. The curves indicate the percentage of the total oxidation for each specie that occurs through the specified reactions at a specific height. The sum of the three reactions at each level is equal to 100 % in all cases. The right panel of each figure shows how much of the specie is oxidized at each level relative to the level of maximum oxidation.

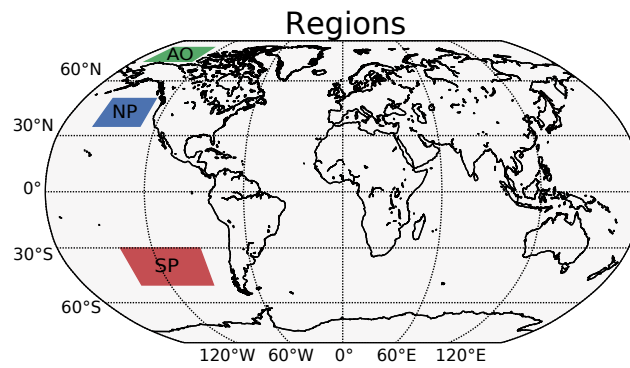


Figure 8. Selected regions with extra focus. AO: Arctic Ocean (70° N - 82° N, 130° W - 170° W). NP: North Pacific (35° N - 50° N, 130° W - 160° W). SP: South Pacific (30° S - 50° S, 90° W - 140° W).

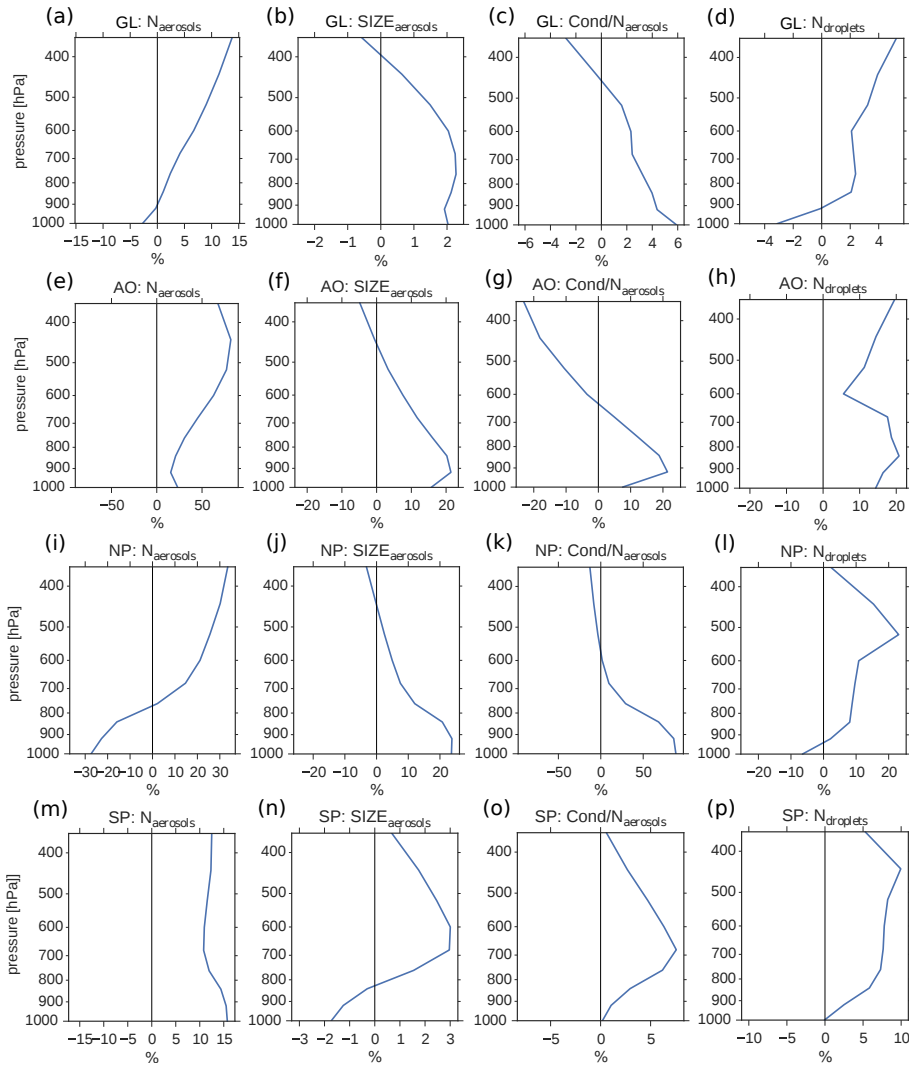


Figure 9. Vertical profiles of annual averaged changes in aerosol number concentration (left), aerosol size (middle left), aerosol condensate divided by the aerosol number concentration (middle right) and CDNC (right) on a global mean (GL) and in the three different regions from Fig. ??-8 (Arctic Ocean (AO), North Pacific (NP) and South Pacific (SP)), when switching from PD- to PI-oxidants in the **PI simulation**. The mean size of the aerosols in the middle left column is calculated as a mean of the number mean radius of all mixtures in the model, weighted by the number of aerosols in each mixture.

The importance of different oxidant reactions at different levels for (a) DMS, (b) SO_2 (c) isoprene and (d) monoterpene. Solid lines: PD-oxidants. Dashed lines: PI-oxidants. The value of a curve at a specific height tells how many percent of the oxidant reactions of that specie happening through the specified reaction. The sum of the three reactions at each level is equal to 100% in each era.

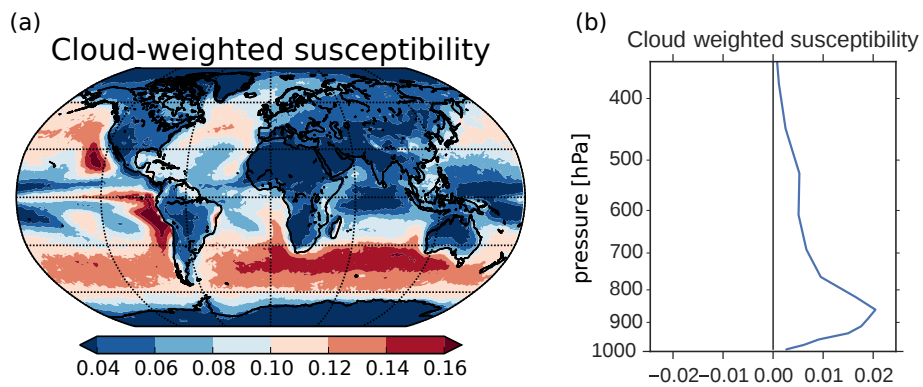


Figure 10. (a) Cloud-weighted susceptibility using Eq. (6) in Alterskjær et al. (2012). Cloud droplet size and numbers from the cloud top layer and the total cloud fraction were applied. (b) Vertical profile of the global mean cloud-weighted susceptibility.

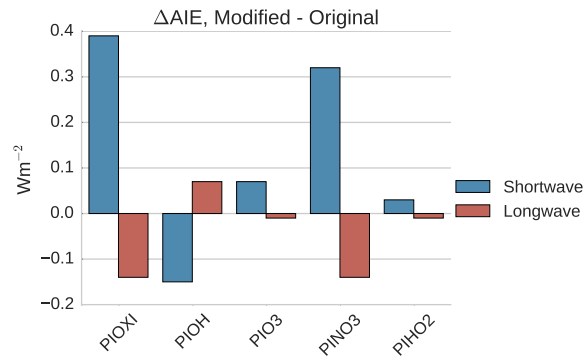


Figure 11. Differences in global mean shortwave and longwave aerosol indirect effect between the setups with modified PI-simulations (PIOXI, PIOH, PINO3 and PIHO2) and the original setup.

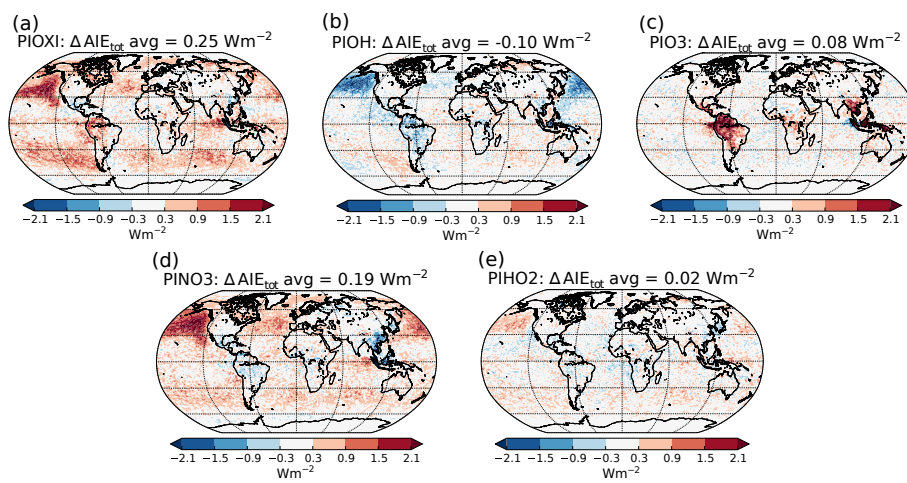


Figure 12. Differences in total aerosol indirect effect between the PI-simulation with (a) PIOXI, (b) PIOH, (c) PIO3, (d) PINO3, (e) PIHO2 and the original PI-simulation with only PD-oxidants.

Table 1. Overview of global emission rates and burdens of the precursor gases in CAM5.3-Oslo. The values come from three different simulations using aerosols and oxidants from present-day, (aerosols from preindustrial and oxidants from present-day), and {aerosols and oxidants from preindustrial}.

<u>Specie</u>	<u>Emission rates [Tg yr⁻¹]</u>	<u>Burdens [Tg]</u>
<u>SO₂</u>	130	0.705
	(29.0)	(0.319)
	{29.0}	{0.380}
<u>DMS</u>	66.3	0.276
	(66.2)	(0.274)
	{66.2}	{0.417}
<u>Isoprene</u>	406	0.148
	(418)	(0.150)
	{417}	{0.287}
<u>Monoterpene</u>	114	0.0358
	(116)	(0.0341)
	{116}	{0.0697}

Table 2. Chemical reactions with corresponding rate coefficients. For (R1), $f_c = 3 \cdot 10^{-31} \cdot \left(\frac{300}{T}\right)^{3.3}$, and $k_{O} = \frac{f_c \cdot M}{1 + (f_c \cdot M \cdot 1.5 \cdot 10^{12})}$, where M is [the number concentration of](#) all molecules that can act as a third body [cm^{-3}]. If the model does not trace an end product of a chemical reaction, the product is lost in the model and not written down in this table, explaining why the [stoichiometry](#) is not exact in all of the reactions.

Reaction number	Reaction	Rate coefficient [$\text{cm}^3 \text{molecule}^{-1} \text{s}^{-1}$]
(R1)	$\text{SO}_2 + \text{OH} + \text{M} \rightarrow \text{H}_2\text{SO}_4 + \text{M}$	$k_O \cdot 0.6 \left(1 + (\log_{10}(f_c \cdot M \cdot 1.5 \cdot 10^{12}))^2\right)^{-1}$
(R2)	$\text{DMS} + \text{OH} \rightarrow \text{SO}_2$	$9.6 \cdot 10^{-12} \cdot e^{-234/T}$
(R3)	$\text{DMS} + \text{OH} \rightarrow 0.75 \cdot \text{SO}_2 + 0.5 \cdot \text{HO}_2 + 0.029 \cdot \text{SOA}_{\text{LV}} + 0.114 \cdot \text{SOA}_{\text{SV}}$	$\frac{(1.7 \cdot 10^{-42} \cdot e^{7810/T} [\text{O}_2])}{(1 + 5.5 \cdot 10^{-31} e^{7460/T} [\text{O}_2])}$
(R4)	$\text{DMS} + \text{NO}_3 \rightarrow \text{SO}_2 + \text{HNO}_3$	$1.9 \cdot 10^{-13} \cdot e^{-520/T}$
(R5)	$\text{monoterpene} + \text{OH} \rightarrow 0.15 \cdot \text{SOA}_{\text{SV}}$	$1.2 \cdot 10^{-11} \cdot e^{-440/T}$
(R6)	$\text{monoterpene} + \text{O}_3 \rightarrow 0.15 \cdot \text{SOA}_{\text{LV}}$	$8.05 \cdot 10^{-16} \cdot e^{-640/T}$
(R7)	$\text{monoterpene} + \text{NO}_3 \rightarrow 0.15 \cdot \text{SOA}_{\text{SV}}$	$1.2 \cdot 10^{-12} \cdot e^{-490/T}$
(R8)	$\text{isoprene} + \text{OH} \rightarrow 0.05 \cdot \text{SOA}_{\text{SV}}$	$2.7 \cdot 10^{-11} \cdot e^{-390/T}$
(R9)	$\text{isoprene} + \text{O}_3 \rightarrow 0.05 \cdot \text{SOA}_{\text{SV}}$	$1.03 \cdot 10^{-14} \cdot e^{-1995/T}$
(R10)	$\text{isoprene} + \text{NO}_3 \rightarrow 0.05 \cdot \text{SOA}_{\text{SV}}$	$3.15 \cdot 10^{-12} \cdot e^{-450/T}$
(R11)	$\text{HO}_2 + \text{HO}_2 \rightarrow \text{H}_2\text{O}_2$	$\left(3.5 \cdot 10^{-13} \cdot e^{430/T} + 1.7 \cdot 10^{-33} \cdot e^{1000/T}\right) \cdot \left(1 + 1.4 \cdot 10^{-21} \cdot [\text{H}_2\text{O}] \cdot e^{2200/T}\right)$
(R12)	$\text{H}_2\text{O}_2 + \text{OH} \rightarrow \text{H}_2\text{O} + \text{HO}_2$	$2.9 \cdot 10^{-12} \cdot e^{-160/T}$
(R13)	$\text{H}_2\text{O}_2 + h\nu \rightarrow 2 \cdot \text{OH}$	

Table 3. Overview of the prescribed precursor- and aerosol emissions and prescribed oxidant concentrations used in the three different simulations that were carried out for each modification to the default model setup.

Name of simulations	Prescribed emissions of aerosols and precursor gases	Prescribed concentrations of oxidants	SSTs, sea-ice extent, greenhouse gases and land use
PDAER_PDOXI_XXX	PD	PD	PD
PIAER_PDOXI_XXX	PI	PD	PD
PIAER_PIOXI_XXX	PI	PI	PD

Table 4. Global mean lifetime of different gaseous and aerosol species (g: gas, a: aerosol) when applying PD- ~~to~~ and PI-oxidants in the PI-simulation. The lifetime is calculated as (Global mean burden)/(Global mean ~~net~~-loss).

Species	Lifetime, PD [h]	Lifetime, PI [h]	Change in lifetime [%]
SO ₂ (g)	29	34	+17
DMS (g)	36	55	+53
Isoprene (g)	3.2	6.0	+88
Monoterpene (g)	2.6	5.3	+104
H ₂ SO ₄ (g)	0.91	1.0	+9.9
SOA _{LV} (g)	0.65	0.82	+26
SOA _{SV} (g)	0.75	1.0	+9.9
SO ₄ (a)	78	84	+7.7
SOA (a)	115	116	+0.9

Table 5. Conversion rates using present-day (preindustrial) oxidants.

<u>Reaction</u>			<u>Loss [Tg yr⁻¹]</u>		<u>Production [Tg yr⁻¹]</u>	
<u>(R2)</u>	DMS + OH	[DMS]	24.0 (31.4)	$\xrightarrow{\sim}$	24.7 (32.4)	[SO ₂]
<u>(R3)</u>	DMS + OH	[DMS]	20.6 (26.7)	$\xrightarrow{0.75}$	16.0 (20.7)	[SO ₂]
				$\xrightarrow{0.029}$	1.62 (2.10)	[SOA _{LV}]
				$\xrightarrow{0.114}$	6.38 (8.26)	[SOA _{SV}]
<u>(R4)</u>	DMS + NO ₃	[DMS]	26.3 (10.4)	$\xrightarrow{\sim}$	27.1 (10.7)	[SO ₂]
<u>(R5)</u>	monoterpene + OH	[monoterpene]	41.3 (50.6)	$\xrightarrow{0.15}$	7.65 (9.37)	[SOA _{SV}]
<u>(R6)</u>	monoterpene + O ₃	[monoterpene]	45.2 (51.4)	$\xrightarrow{0.15}$	8.38 (9.53)	[SOA _{LV}]
<u>(R7)</u>	monoterpene + NO ₃	[monoterpene]	32.8 (12.7)	$\xrightarrow{0.15}$	6.09 (2.36)	[SOA _{SV}]
<u>(R8)</u>	isoprene + OH	[isoprene]	376 (376)	$\xrightarrow{0.05}$	46.4 (46.4)	[SOA _{SV}]
<u>(R9)</u>	isoprene + O ₃	[isoprene]	26.7 (27.6)	$\xrightarrow{0.05}$	3.30 (3.41)	[SOA _{SV}]
<u>(R10)</u>	isoprene + NO ₃	[isoprene]	21.8 (6.72)	$\xrightarrow{0.05}$	2.70 (0.830)	[SOA _{SV}]
<u>(R2)</u>	SO ₂ + OH + M	[SO ₂]	10.4 (10.1)	$\xrightarrow{\sim}$	16.0 (15.5)	[H ₂ SO ₄]
<u>(aq)</u>	SO ₂ + O ₃	[SO ₂]	14.6 (14.8)	$\xrightarrow{\sim}$	21.9 (22.3)	[SO ₄]
<u>(aq)</u>	SO ₂ + H ₂ O ₂	[SO ₂]	28.4 (22.5)	$\xrightarrow{\sim}$	42.6 (33.7)	[SO ₄]
	SO ₂ <u>dry deposition</u>	[SO ₂]	16.5 (16.5)			
	SO ₂ <u>wet deposition</u>	[SO ₂]	22.5 (25.4)			

Table 6. Difference in global mean SW and LW indirect effects between setups with the modified PI-simulation in the second column and the default PI-simulation with PD-oxidants. The bottom row shows the effect of changing all of the oxidants at a the same time (similar to Figure ??Fig. 3(c,d)), the other odd numbered rows show the effect of changing one oxidant at a the time in the PI-simulation, while the even numbered rows show the difference in switching all oxidants (PIOXI) and all but one (PIOXI_PDXXX) in the PI-simulation.

Row number	Description of the modified PI-simulation	Change in shortwave aerosol indirect effect [Wm^{-2}]	Change in longwave aerosol indirect effect [Wm^{-2}]
1	PDOXI_PIOH	-0.15	+0.07
2	PIOXI – PIOXI_PDOH	-0.06	+0.02
3	PDOXI_PIO3	+0.07	-0.01
4	PIOXI – PIOXI_PDO3	+0.12	0.00
5	PDOXI_PINO3	+0.32	-0.14
6	PIOXI – PIOXI_PDNO3	+0.41	-0.11
7	PDOXI_PIH02	+0.03	-0.01
8	PIOXI – PIOXI_PDHO2	+0.03	+0.01
9	PIOXI	+0.39	-0.14

Table 7. Information about how the setup for the sensitivity tests deviate-deviates from the default original setup. The right column shows how the total aerosol indirect effect changes when switching from PD- to PI-oxidants in the PI-simulation. ΔAIE_{tot} with the default model setup was $+0.25 \text{ Wm}^{-2}$

Name of simulations	Description of setup	<u>$\Delta AIE_{tot} [\text{Wm}^{-2}]$</u>
NOSOALVDMS	None of the SOA produced through (R3) is allowed to nucleate new particles. (R3) is thus replaced with $\text{DMS} + \text{OH} \rightarrow 0.75 \cdot \text{SO}_2 + 0.5 \cdot \text{HO}_2 + 0.143 \cdot \text{SOA}_{SV}$	<u>+0.25</u>
NOSOALVBVOC	None of the SOA produced through (R6) is allowed to nucleate new particles. (R6) is thus replaced with $\text{monoterpene} + \text{O}_3 \rightarrow 0.15 \cdot \text{SOA}_{SV}$	<u>+0.26</u>
NOSOA	No SOA production from DMS-oxidation. (R3) is thus replaced with $\text{DMS} + \text{OH} \rightarrow 0.75 \cdot \text{SO}_2 + 0.5 \cdot \text{HO}_2$	<u>+0.14</u>
NACTOFF	No activation from particle mixture number 1 (Kirkevåg et al., 2018). This mixture corresponds to the nucleation mode in modal aerosol schemes, and this is where we find the newly formed SOA- and SO ₄ -aerosols.	<u>-0.03</u>
<u>DIURNALNO3</u>	Add a daily cycle to the concentrations of NO ₃ that come from prescribed, monthly mean values.	<u>+0.26</u>
<u>FREEMET</u>	Apply free meteorology instead of nudged winds.	<u>+0.3 ± 0.2</u>